Binary black holes: formation and observations

Isaak Markovich Khalatnikov

Centennial

Landau ITP, October 19, 2019

Konstantin Postnov
SAI MSU
Faculty of Physics, MSU

(In collaboration with A. Kuranov, N. Mitichkin (MSU), I. Simkin (Bauman MTU))

Plan

- Binary black holes from current GW observations – confirmed expectations anf unexpected features
- Astrophysical binary BHs
- EM from binary BH+NS
- Primordial binary BHs

GW from coalescing compact binaries

- Waveform from two coalescing point-like masses is determined by a combination of component masses (the chirp mass)

$$M_{ch} = (\mu^3 M^2)^{1/5}$$

$$h \sim M_{ch}^{5/3} f^{2/3} / r$$

$$\mathcal{M} = \frac{(m_1 m_2)^{3/5}}{(m_1 + m_2)^{1/5}} = \frac{c^3}{G}\left(\frac{5}{96}\pi^{-8/3} f^{-11/3} \dot{f}\right)^{3/5}$$

LIGO
Hanford
USA

KAGRA
Kamioka
Japan

Virgo
Pisa
Italy

LIGO
Livingston
USA

Credit: LVC collab., Univ. of Tokyo

Current status of GW interferometers

- O3 LIGO/Virgo/GEO-600: April 1-October 3 2019
- Commissioning break since October 3 (~month)
- KAGRA underground GW interferometer started commissioning run on October 4, 2019

Current Detection horizon

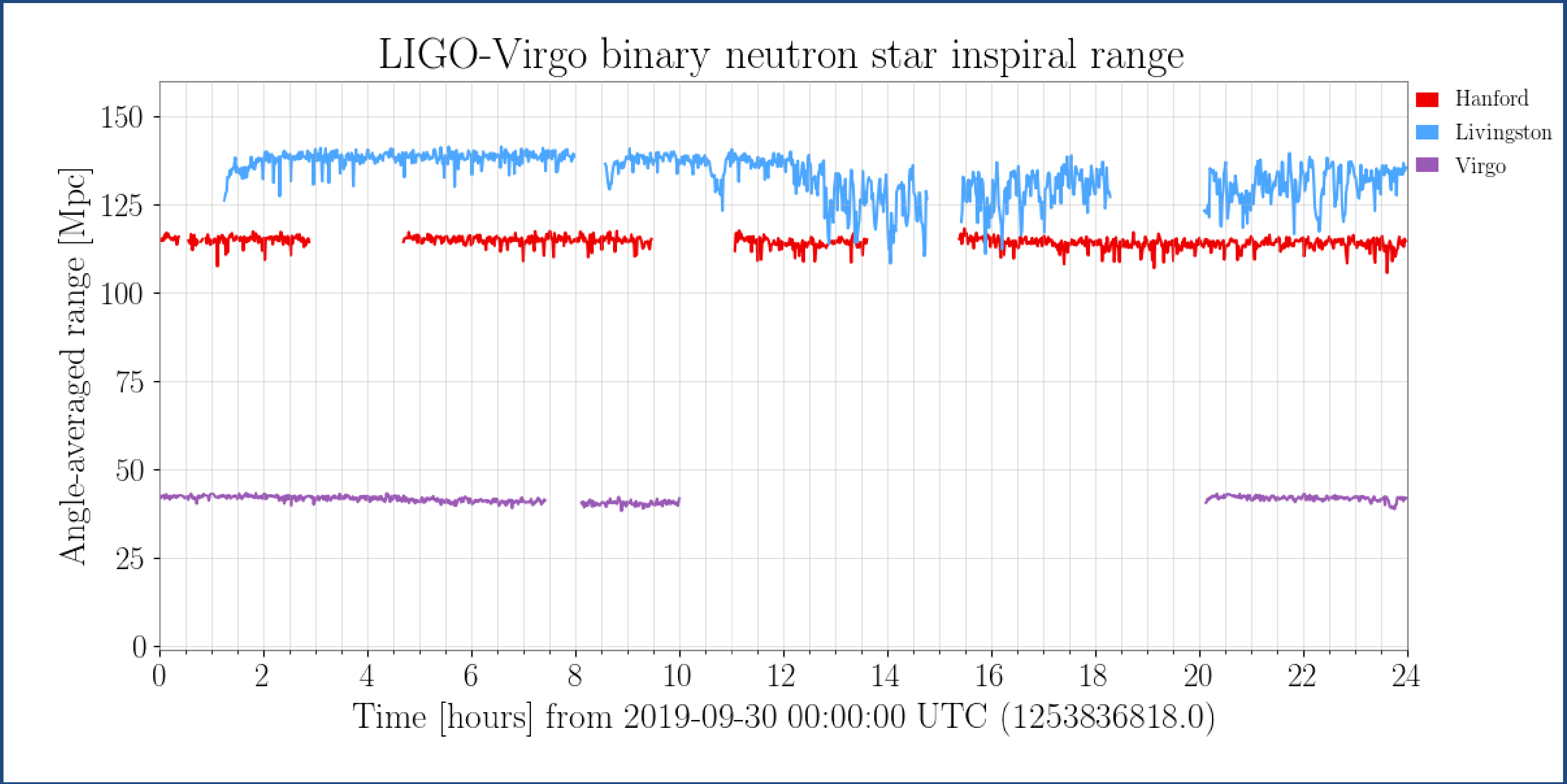

$D_h \sim M_{chirp}^{5/6}$

https://www.gw-openscience.org/

LVC O3 detections

- 33 triggers, 21 BH+BH, 3 NS+NS, 4 NS+BH candidates

  https://gracedb.ligo.org

- No electromagnetic counterparts so far

GW 150914 template vs observations: 94(+2/-3)%

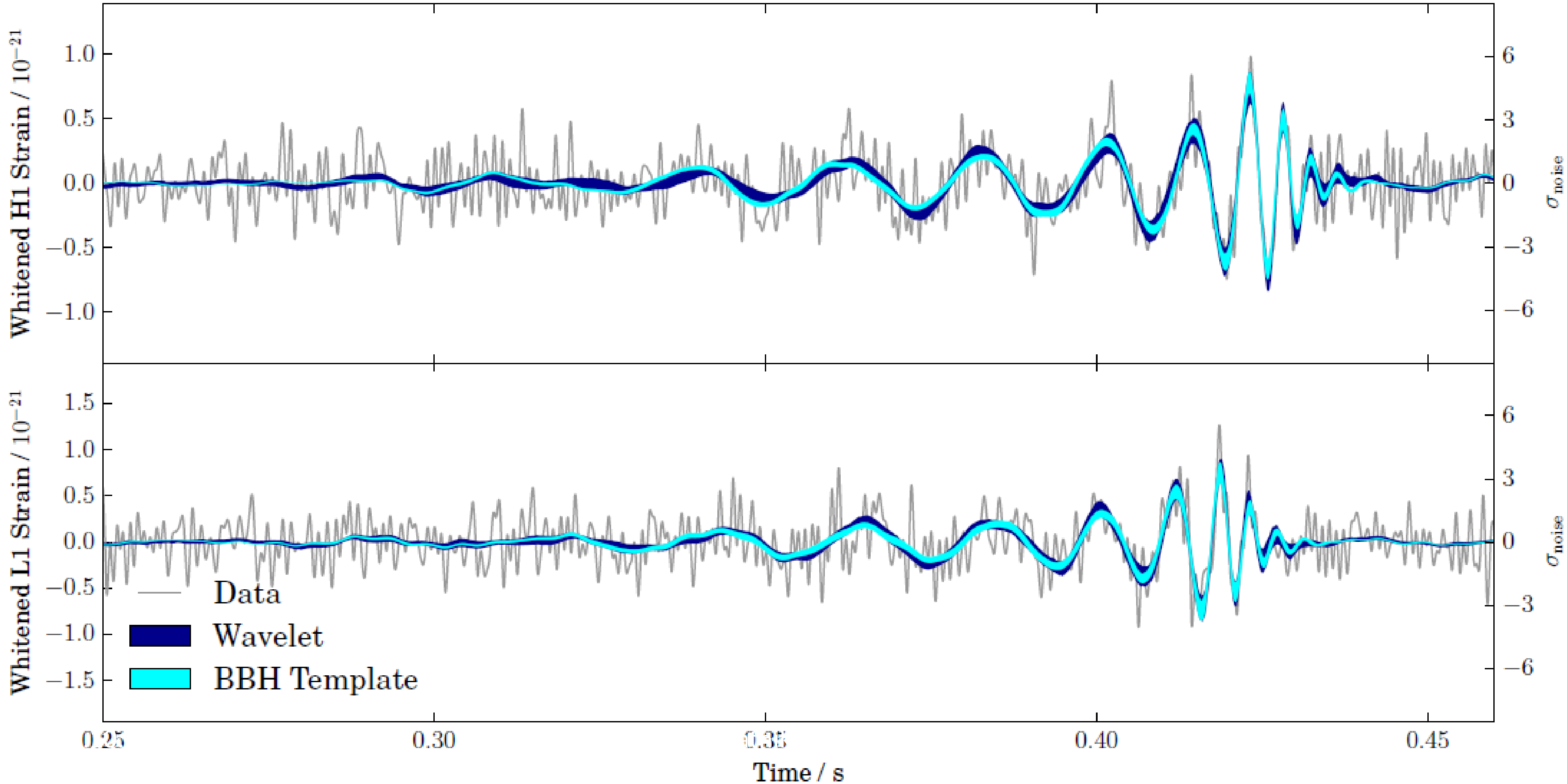

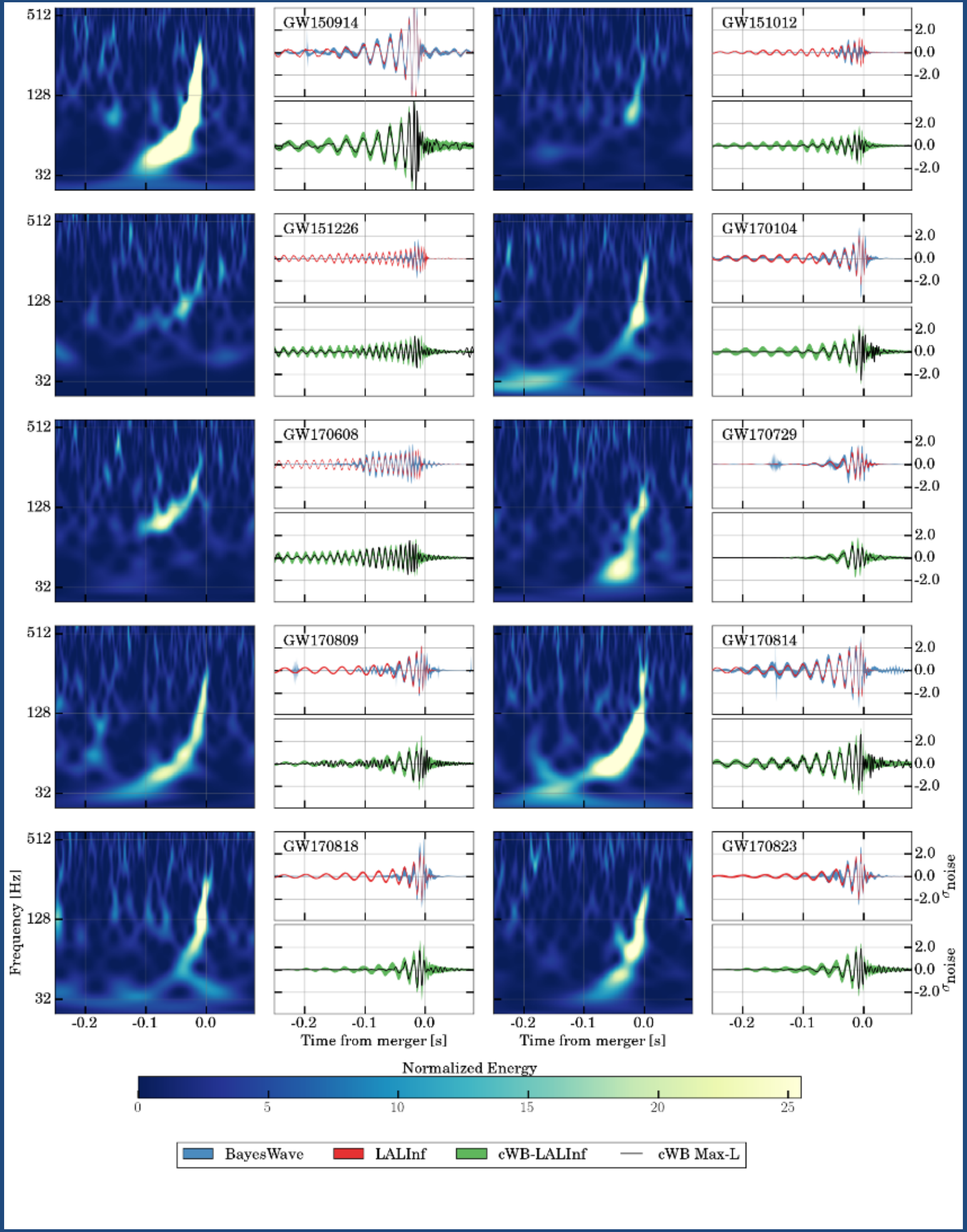

LIGO BHs

GWTC-1 Catalog arXiv:1811.12907

Parameters from GW observations

$$\mathcal{M} = \frac{(m_1 m_2)^{3/5}}{M^{1/5}}$$

Chirp mass

$$\chi_{\text{eff}} = \frac{(m_1 \vec{\chi}_1 + m_2 \vec{\chi}_2) \cdot \hat{L}_N}{M}$$

Effective spin

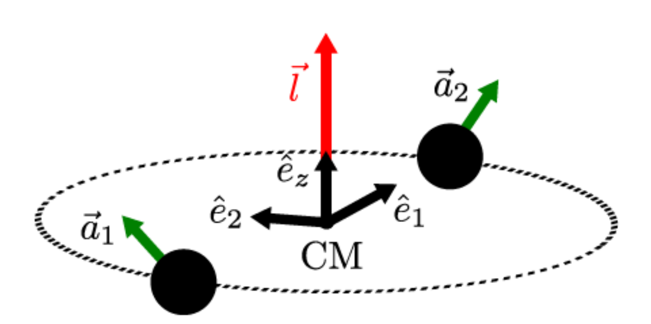

Event	$m_1/\mathrm{M}_\odot$	$m_2/\mathrm{M}_\odot$	$\mathcal{M}/\mathrm{M}_\odot$	χ_{eff}	$M_{\mathrm{f}}/\mathrm{M}_\odot$	a_{f}	$E_{\mathrm{rad}}/(\mathrm{M}_\odot c^2)$	$\ell_{\mathrm{peak}}/(\mathrm{erg\,s^{-1}})$	d_L/Mpc	z	$\Delta\Omega/\mathrm{deg}^2$
GW150914	$35.6^{+4.8}_{-3.0}$	$30.6^{+3.0}_{-4.4}$	$28.6^{+1.6}_{-1.5}$	$-0.01^{+0.12}_{-0.13}$	$63.1^{+3.3}_{-3.0}$	$0.69^{+0.05}_{-0.04}$	$3.1^{+0.4}_{-0.4}$	$3.6^{+0.4}_{-0.4} \times 10^{56}$	430^{+150}_{-170}	$0.09^{+0.03}_{-0.03}$	180
GW151012	$23.3^{+14.0}_{-5.5}$	$13.6^{+4.1}_{-4.8}$	$15.2^{+2.0}_{-1.1}$	$0.04^{+0.28}_{-0.19}$	$35.7^{+9.9}_{-3.8}$	$0.67^{+0.13}_{-0.11}$	$1.5^{+0.5}_{-0.5}$	$3.2^{+0.8}_{-1.7} \times 10^{56}$	1060^{+540}_{-480}	$0.21^{+0.09}_{-0.09}$	1555
GW151226	$13.7^{+8.8}_{-3.2}$	$7.7^{+2.2}_{-2.6}$	$8.9^{+0.3}_{-0.3}$	$0.18^{+0.20}_{-0.12}$	$20.5^{+6.4}_{-1.5}$	$0.74^{+0.07}_{-0.05}$	$1.0^{+0.1}_{-0.2}$	$3.4^{+0.7}_{-1.7} \times 10^{56}$	440^{+180}_{-190}	$0.09^{+0.04}_{-0.04}$	1033
GW170104	$31.0^{+7.2}_{-5.6}$	$20.1^{+4.9}_{-4.5}$	$21.5^{+2.1}_{-1.7}$	$-0.04^{+0.17}_{-0.20}$	$49.1^{+5.2}_{-3.9}$	$0.66^{+0.08}_{-0.10}$	$2.2^{+0.5}_{-0.5}$	$3.3^{+0.6}_{-0.9} \times 10^{56}$	960^{+430}_{-410}	$0.19^{+0.07}_{-0.08}$	924
GW170608	$10.9^{+5.3}_{-1.7}$	$7.6^{+1.3}_{-2.1}$	$7.9^{+0.2}_{-0.2}$	$0.03^{+0.19}_{-0.07}$	$17.8^{+3.2}_{-0.7}$	$0.69^{+0.04}_{-0.04}$	$0.9^{+0.05}_{-0.1}$	$3.5^{+0.4}_{-1.3} \times 10^{56}$	320^{+120}_{-110}	$0.07^{+0.02}_{-0.02}$	396
GW170729	$50.6^{+16.6}_{-10.2}$	$34.3^{+9.1}_{-10.1}$	$35.7^{+6.5}_{-4.7}$	$0.36^{+0.21}_{-0.25}$	$80.3^{+14.6}_{-10.2}$	$0.81^{+0.07}_{-0.13}$	$4.8^{+1.7}_{-1.7}$	$4.2^{+0.9}_{-1.5} \times 10^{56}$	2750^{+1350}_{-1320}	$0.48^{+0.19}_{-0.20}$	1033
GW170809	$35.2^{+8.3}_{-6.0}$	$23.8^{+5.2}_{-5.1}$	$25.0^{+2.1}_{-1.6}$	$0.07^{+0.16}_{-0.16}$	$56.4^{+5.2}_{-3.7}$	$0.70^{+0.08}_{-0.09}$	$2.7^{+0.6}_{-0.6}$	$3.5^{+0.6}_{-0.9} \times 10^{56}$	990^{+320}_{-380}	$0.20^{+0.05}_{-0.07}$	340
GW170814	$30.7^{+5.7}_{-3.0}$	$25.3^{+2.9}_{-4.1}$	$24.2^{+1.4}_{-1.1}$	$0.07^{+0.12}_{-0.11}$	$53.4^{+3.2}_{-2.4}$	$0.72^{+0.07}_{-0.05}$	$2.7^{+0.4}_{-0.3}$	$3.7^{+0.4}_{-0.5} \times 10^{56}$	580^{+160}_{-210}	$0.12^{+0.03}_{-0.04}$	87
GW170817	$1.46^{+0.12}_{-0.10}$	$1.27^{+0.09}_{-0.09}$	$1.186^{+0.001}_{-0.001}$	$0.00^{+0.02}_{-0.01}$	≤ 2.8	≤ 0.89	≥ 0.04	$\geq 0.1 \times 10^{56}$	40^{+10}_{-10}	$0.01^{+0.00}_{-0.00}$	16
GW170818	$35.5^{+7.5}_{-4.7}$	$26.8^{+4.3}_{-5.2}$	$26.7^{+2.1}_{-1.7}$	$-0.09^{+0.18}_{-0.21}$	$59.8^{+4.8}_{-3.8}$	$0.67^{+0.07}_{-0.08}$	$2.7^{+0.5}_{-0.5}$	$3.4^{+0.5}_{-0.7} \times 10^{56}$	1020^{+430}_{-360}	$0.20^{+0.07}_{-0.07}$	39
GW170823	$39.6^{+10.0}_{-6.6}$	$29.4^{+6.3}_{-7.1}$	$29.3^{+4.2}_{-3.2}$	$0.08^{+0.20}_{-0.22}$	$65.6^{+9.4}_{-6.6}$	$0.71^{+0.08}_{-0.10}$	$3.3^{+0.9}_{-0.8}$	$3.6^{+0.6}_{-0.9} \times 10^{56}$	1850^{+840}_{-840}	$0.34^{+0.13}_{-0.14}$	1651

arXiv:1811.12907

LIGO BH: Masses

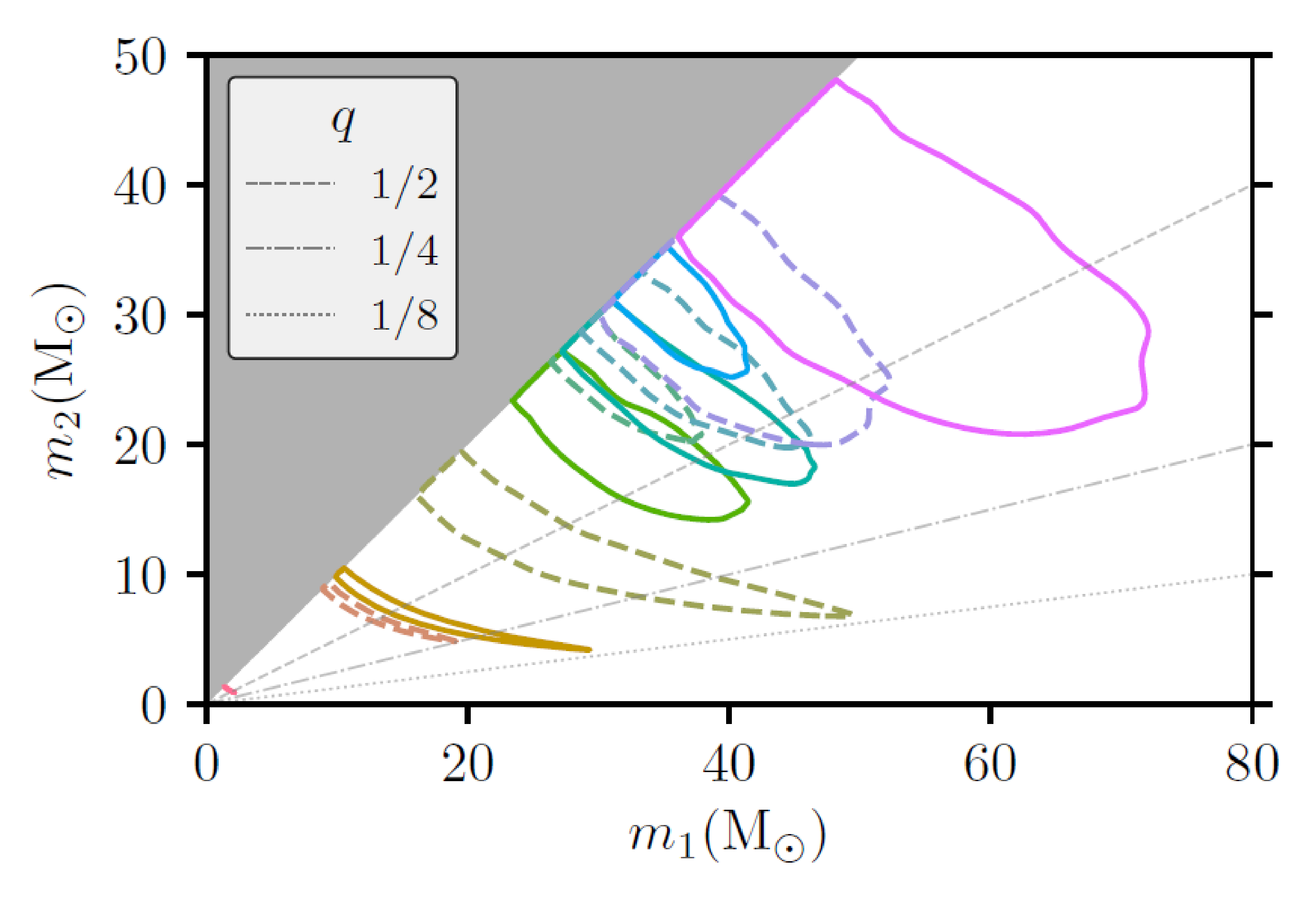

LIGO BH: effective spins

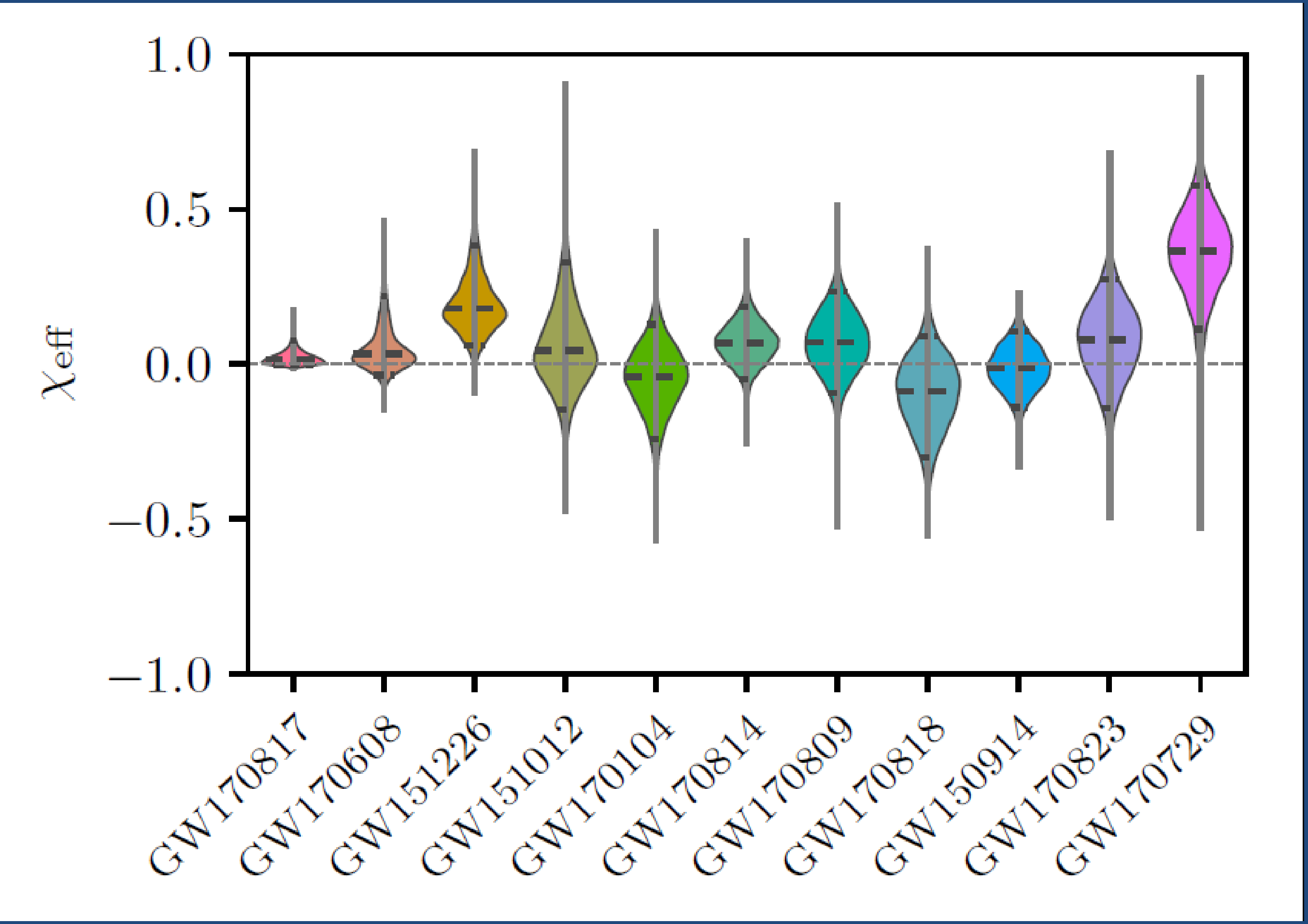

Corollary:

- Larger masses (compared to BHs in XRBs)
- Low effective spins (but GW170729 and possibly GW151226)

1. Astrophysical binary BHs

- BH formation
  - Initial ZAMS mass
  - Initial rotation
  - Possible kick
- BH in binaries
  - From massive binary systems
  - In dense stellar clusters (dynamical)
  - Primordial BHs

BH formation from stars (solar metallicity)

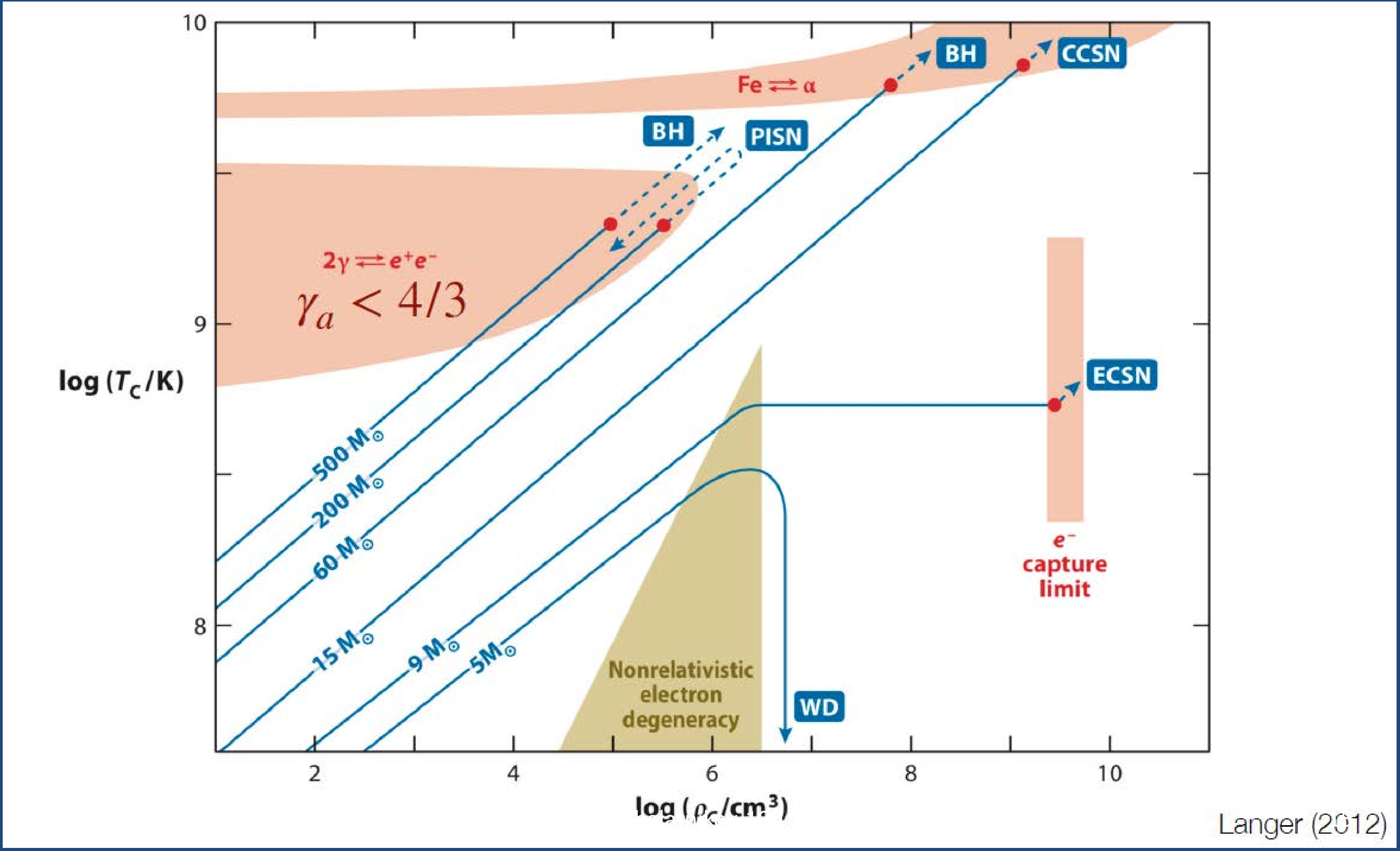

Dependence on the metallicity and stellar wind mass loss

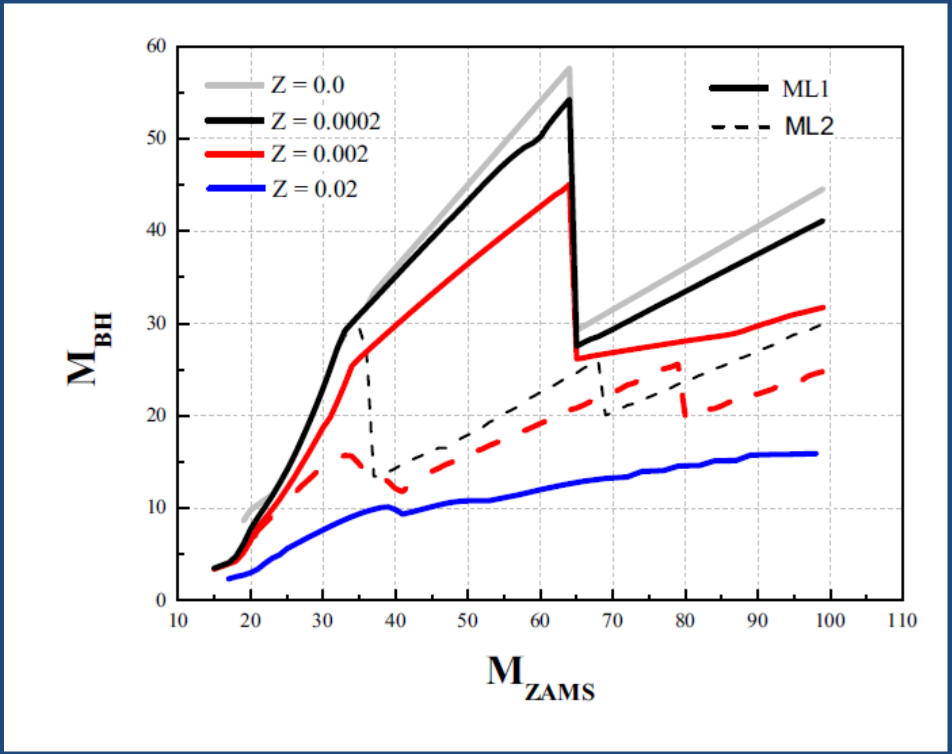

Fryer et al 2012, Giacobbo et al. 2018

PPISN prohibits formation of BH more massive than ~60 $M_\odot$

Binary BH formation

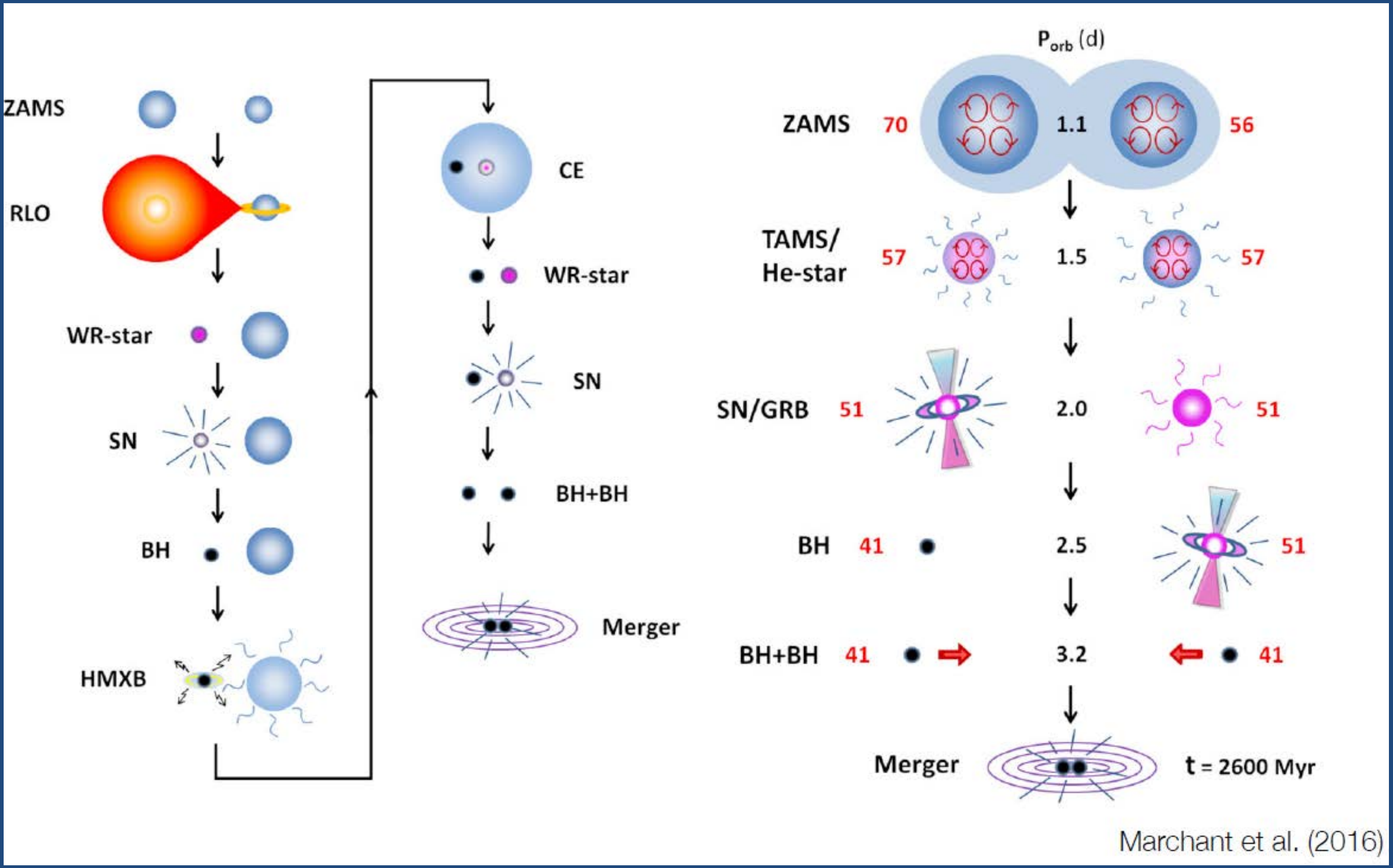

Additional effects in binaries:

- Initial spin misalignment
- Tidal synchronization of the envelope
- Common envelope phase
- Star formation and metallicity history in galaxies

$$\Psi\left(z, \frac{Z}{Z_\odot}\right) = \psi(z)\Phi(Z/Z_\odot),$$

$$\Phi(Z/Z_\odot) = \frac{\hat{\Gamma}[0.84, (Z/Z_\odot)^2\, 10^{0.3z}]}{\Gamma(0.84)}$$

Predictions and surprises

- Binary BH+BH coalescences must be much more numerous and should be detected first (Tutukov, Yungelson 1993, Lipunov, Postnov, Prokhorov 1997,….confirmed!)
- Mass of BH in LIGO binaries is up to ~50 $M_\odot$ (surprise, but can be reconciled with stellar evolution), rumors that a 100 $M_\odot$ was found in O3 (tbc) (a puzzle for stellar evolution – zero-metallicity PopIII stars?)
- Low effective spins (surprise, but can be reconciled with binary evolution) (PK+'19, Fuller+19)

BH+BH mass and spin distributions before coalescence

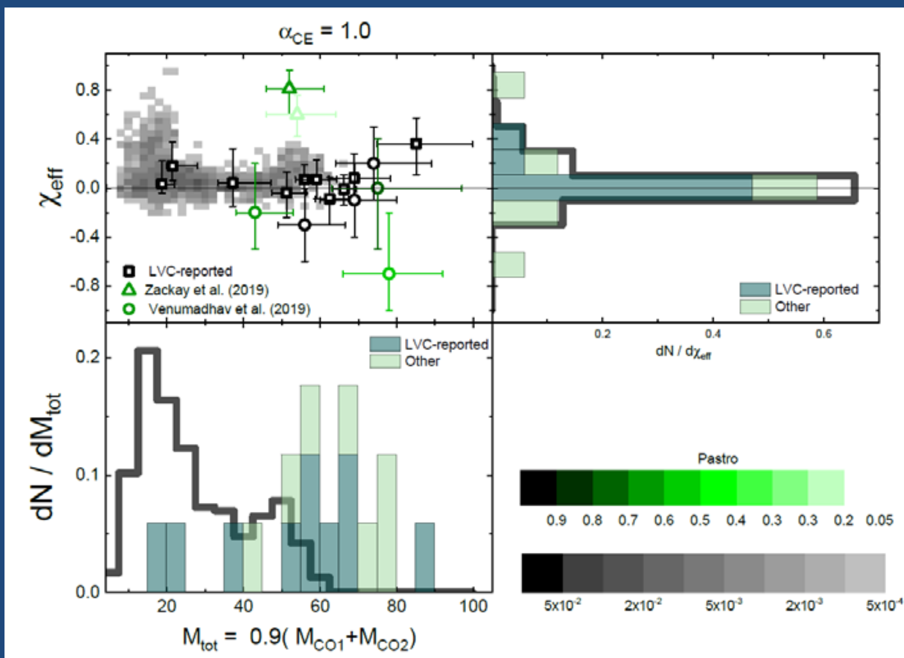

Without fallback

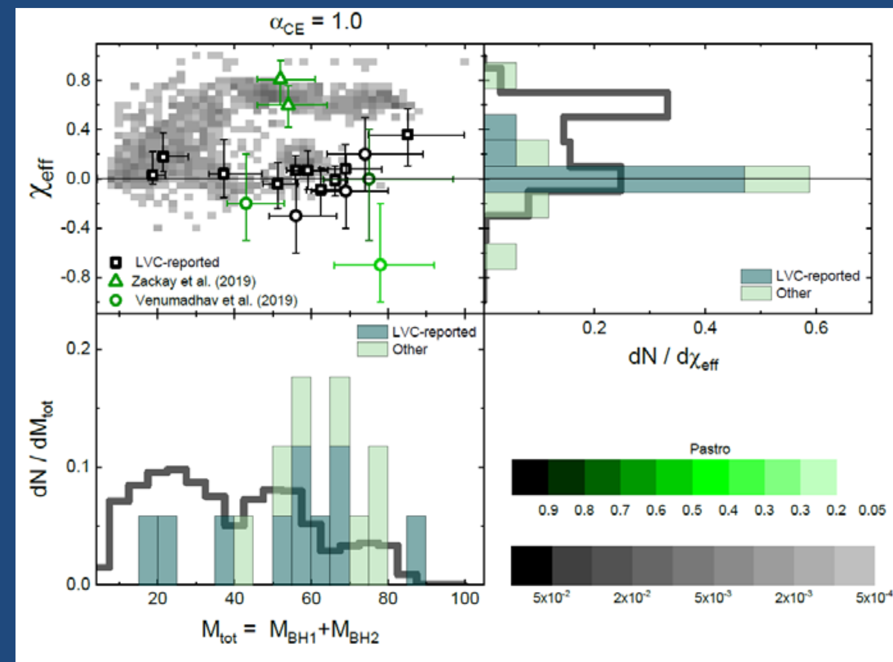

+ fallback from envelope

PK+ 2019, Physics-Uspekhi (2019, No 11, in press)

MNRAS 483, 3288–3306 (2019)

Table 2. Candidate events in the full search of O1 and O2 data. Candidates are sorted by FAR evaluated for the entire b
of templates. Note that ranking statistic and false alarm rate may not have a strictly monotonic relationship due to var
data quality between sub-analyses. The mass and spin parameters listed are associated with the template waveform yiel
the highest ranked multi-detector event for each candidate, and may differ significantly from full Bayesian parameter estima
Masses are quoted in detector frame, and are thus larger than source frame masses by a factor $(1 + z)$, where z is the so
redshift.

Date designation	GPS time	FAR^{-1} (y)	Detectors	$\tilde{\Lambda}$	ρ_H	ρ_L	ρ_V	m_1	m_2	χ_{eff}
170817+12:41:04UTC	1187008882.45	> 10000	HL	180.46	18.6	24.3	-	1.5	1.3	-0.00
150914+09:50:45UTC	1126259462.43	> 10000	HL	93.82	19.7	13.4	-	44.2	32.2	0.09
170104+10:11:58UTC	1167559936.60	> 10000	HL	35.54	9.0	9.6	-	47.9	16.0	0.03
170823+13:13:58UTC	1187529256.52	> 10000	HL	55.04	6.3	9.2	-	68.9	47.2	0.23
170814+10:30:43UTC	1186741861.54	> 10000	HL	52.85	9.0	13.0	-	58.7	23.3	0.53
151226+03:38:53UTC	1135136350.65	> 10000	HL	42.90	10.7	7.4	-	14.8	8.5	0.24
170809+08:28:21UTC	1186302519.76	9400	HL	40.59	6.6	10.7	-	36.0	33.7	0.07
170608+02:01:16UTC	1180922494.49	> 910[a]	HL	51.01	12.5	8.7	-	16.8	6.1	0.31
151012+09:54:43UTC	1128678900.45	220	HL	20.18	7.0	6.7	-	30.8	12.9	-0.05
170729+18:56:29UTC	1185389807.33	6.4	HL	15.33	7.4	6.7	-	106.5	49.7	0.59
170121+21:25:36UTC	1169069154.58	1.3	HL	15.76	5.1	8.7	-	40.4	13.6	-0.98
170727+01:04:30UTC	1185152688.03	.53	HL	13.75	4.5	6.9	-	65.2	26.5	-0.35
170818+02:25:09UTC	1187058327.09	.22	HL	13.29	4.4	9.4	-	53.7	27.4	0.07
170722+08:45:14UTC	1184748332.91	.11	HL	12.19	5.0	6.4	-	248.1	7.1	0.99
170321+03:13:21UTC	1174101219.23	.1	HL	12.22	6.5	6.4	-	11.0	1.3	-0.89
170310+09:30:52UTC	1173173470.77	.07	HL	12.15	6.1	6.2	-	2.1	1.1	-0.20
170809+03:55:52UTC	1186286170.08	.07	LV	7.34	-	7.0	5.1	6.2	1.2	0.60
170819+07:30:53UTC	1187163071.23	.05	HV	11.35	6.3	-	6.7	135.2	2.5	0.85
170618+20:00:39UTC	1181851257.72	.05	HL	11.49	5.2	6.7	-	2.9	2.1	0.30
170416+18:38:48UTC	1176403146.15	.04	HL	11.21	5.1	6.9	-	7.8	1.1	-0.47
170331+07:08:18UTC	1174979316.31	.04	HL	11.03	5.2	7.0	-	3.9	1.1	-0.34
151216+18:49:30UTC	1134326987.60	.04	HL	11.54	6.1	6.0	-	13.9	5.0	-0.41
170306+04:45:50UTC	1172810768.08	.04	HL	11.47	4.8	7.3	-	26.4	1.8	0.23
151227+16:52:22UTC	1135270359.27	.04	HL	11.75	7.3	4.6	-	154.5	4.9	1.00
170126+23:56:22UTC	1169510200.17	.04	HL	11.61	6.4	5.7	-	4.9	1.3	0.79
151202+01:18:13UTC	1133054310.55	.03	HL	11.48	6.5	5.7	-	40.4	1.8	-0.26
170208+20:23:00UTC	1170620598.15	.03	HL	11.12	6.8	5.4	-	6.9	1.0	0.09
170327+17:07:35UTC	1174669673.72	.03	HL	10.65	6.0	6.2	-	40.1	1.0	0.97
170823+13:40:55UTC	1187530873.86	.03	LV	9.30	-	8.0	5.8	117.9	1.3	0.98
150928+10:49:00UTC	1127472557.93	.03	HL	11.28	6.0	6.3	-	2.5	1.0	-0.70

New candidates from O1 and O2

1910.05331

Independent detections: a new trend?

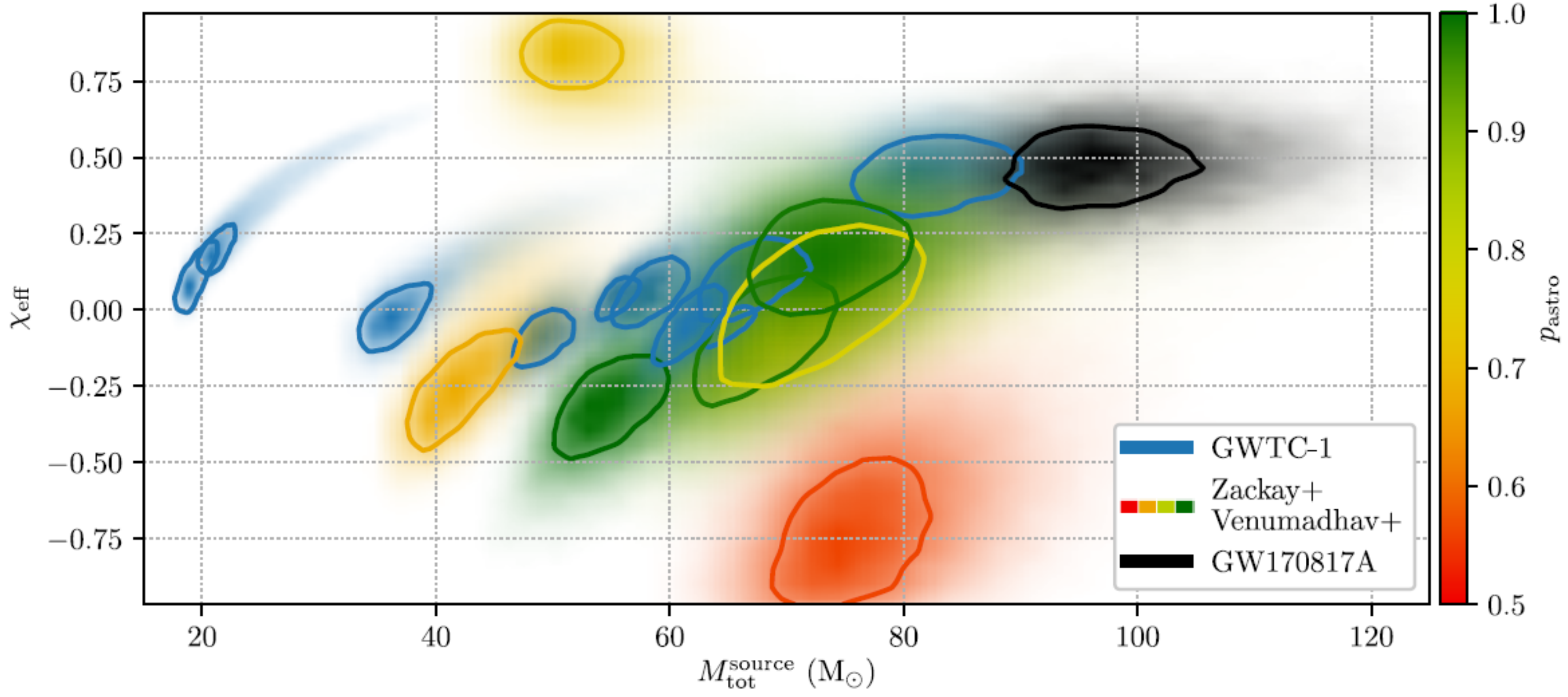

FIG. 7: Binary black holes events reported from O1 and O2, in the plane of source-frame total mass vs. effective spin. In blue are shown the 10 BBH events reported in GWTC-1 [1], all of them are certainly astrophysical in origin ($p_{\text{astro}} = 1$). Color coded by p_{astro} are shown 7 additional events with $p_{\text{astro}} > 0.5$ that our previous searches found [2, 4]. In black we show GW170817A. Displayed are 1σ probability contours, i.e. enclosing $1 - e^{-1/2} \approx 0.39$ of the probability distribution.

1910.09528

2. BH+NS systems

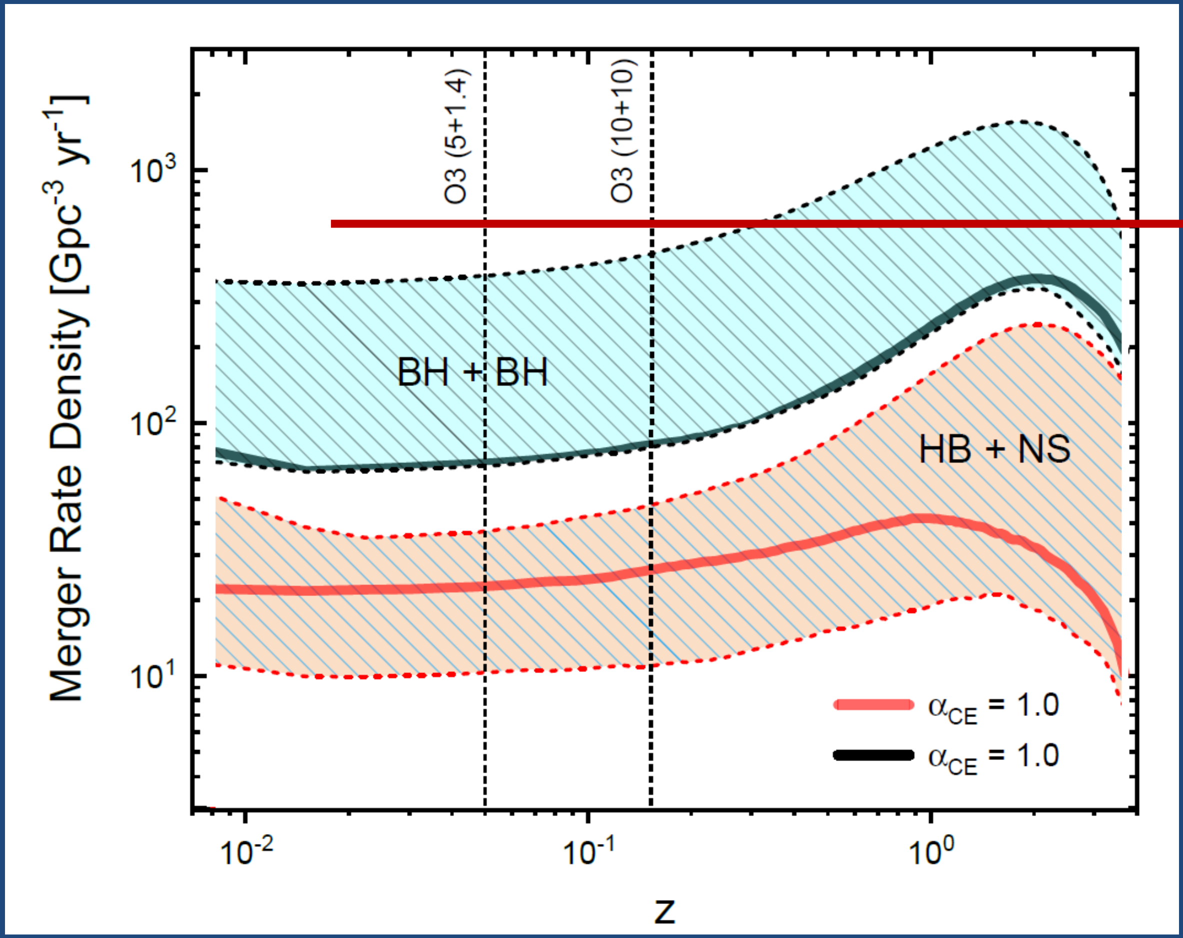

NS+BH upper limit
610 Gpc^{-3} yr^{-1}

1811.12907

PK+ 2019, Physics-Uspekhi (2019, No 11, in press); 1907.04218

Detection rate BH+BH, BH+NS

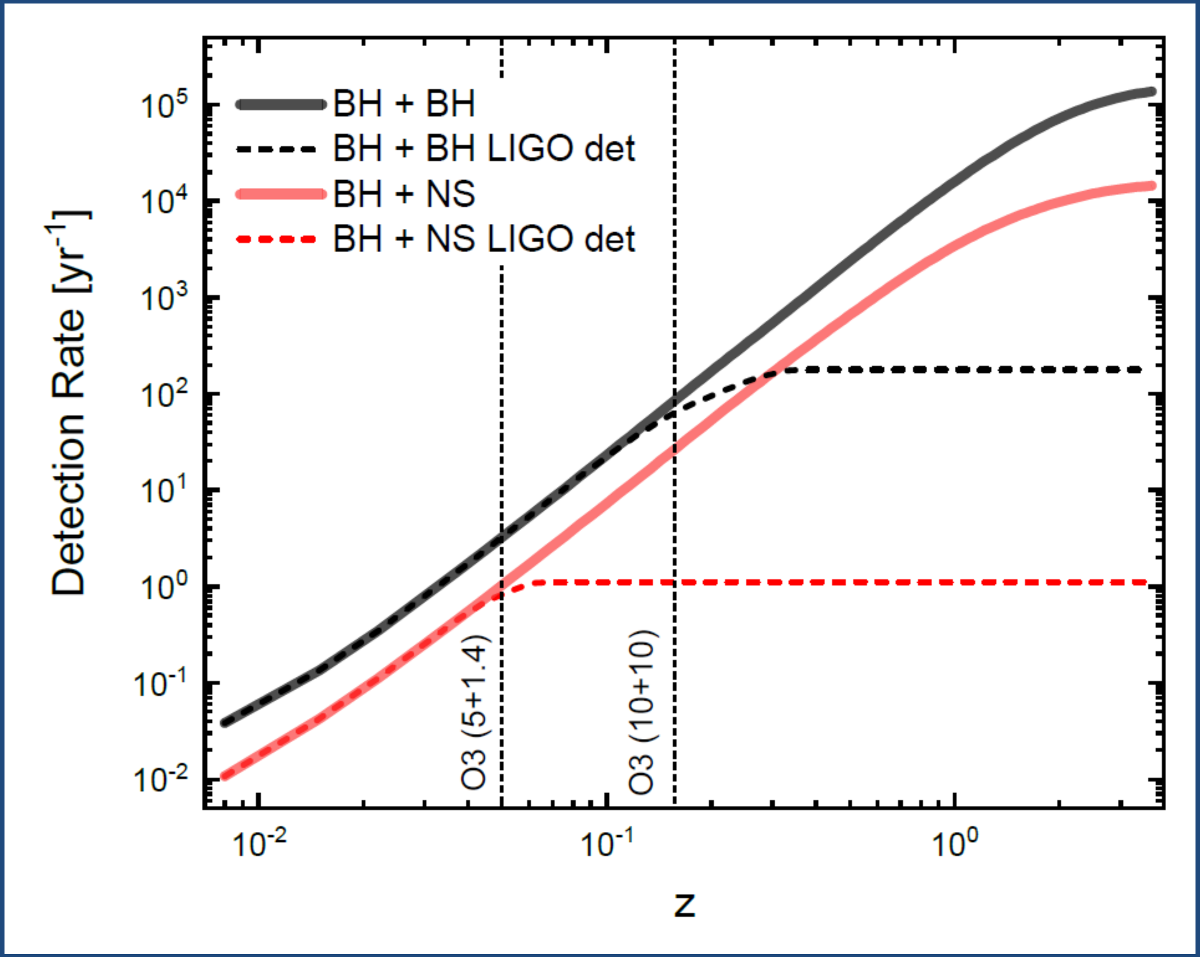

 1907.04218

EM emission from NS+BH

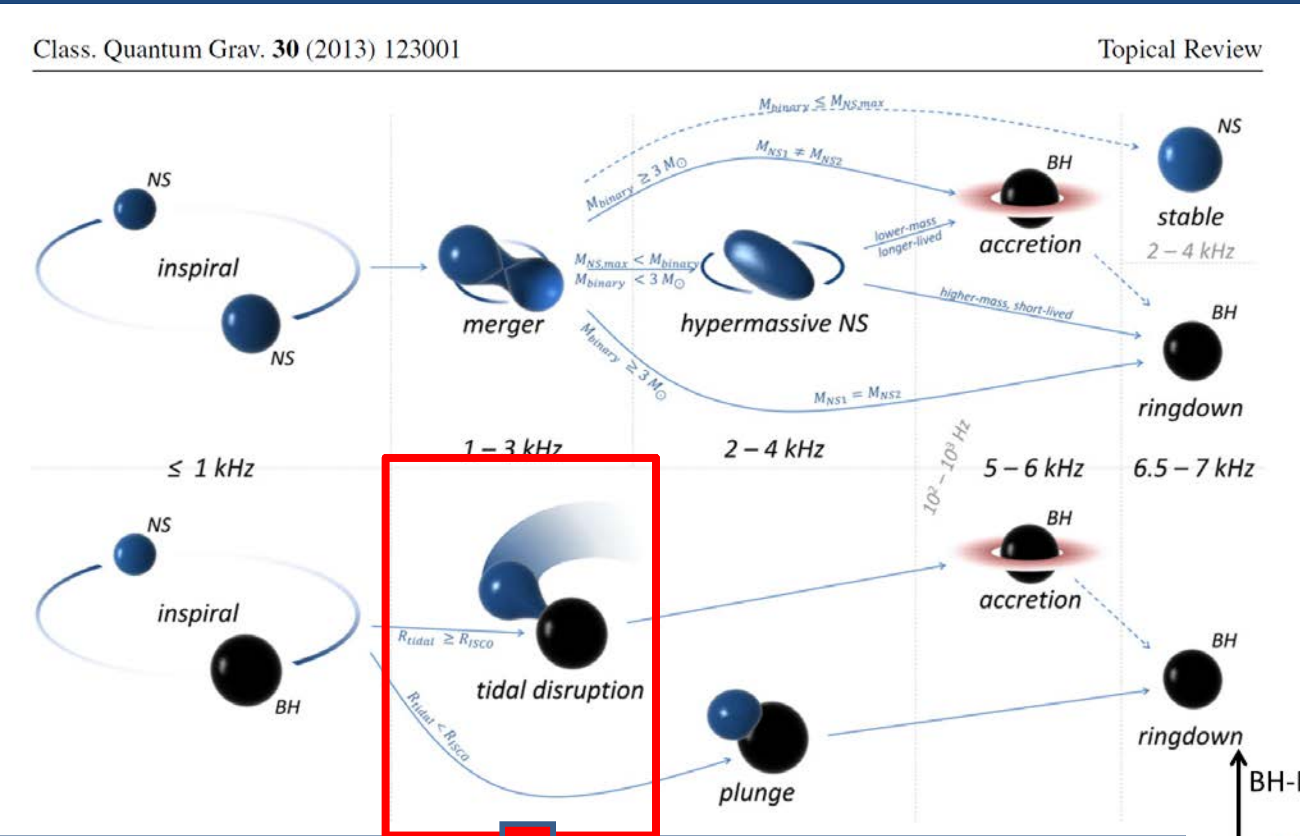

EM-favorable

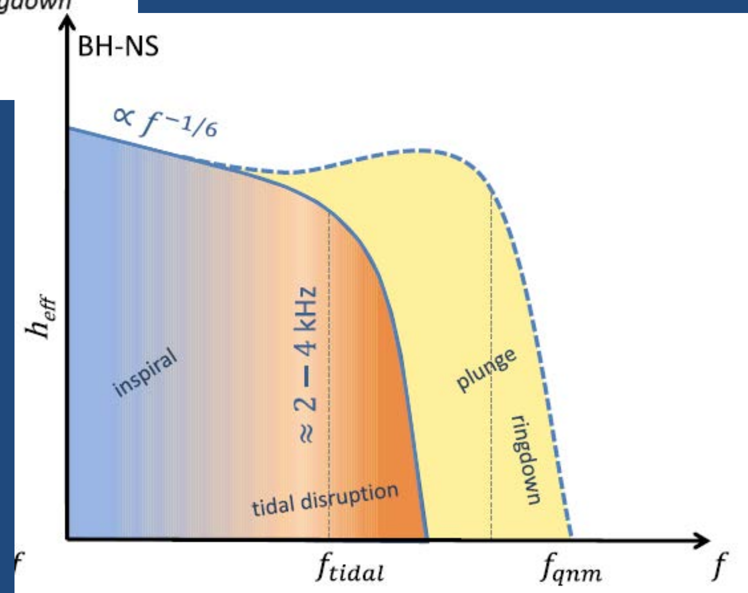

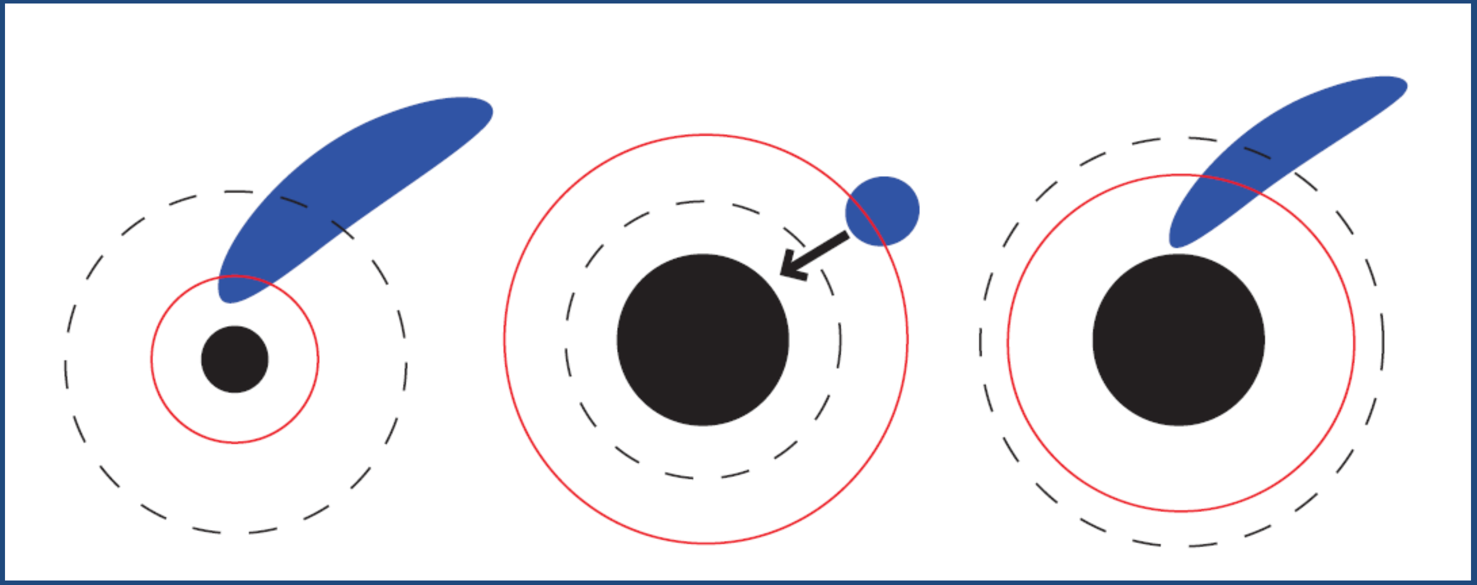

$R_{tid} > R_{ISCO}$ $R_{tid} < R_{ISCO}$ $R_{tid} \sim R_{ISCO}$

Kyotoku+'11

Mass shedding and tidal disruption

$$r_{\rm ISCO}/M = 3 + Z_2 \mp \sqrt{(3 - Z_1)(3 + Z_1 + 2Z_2)}$$
$$Z_1 \equiv 1 + (1 - \chi_1^2)^{1/3} \times \left[(1 + \chi_1)^{1/3} + (1 - \chi_1)^{1/3}\right]$$
$$Z_2 \equiv \sqrt{3\chi_1^2 + Z_1^2}$$

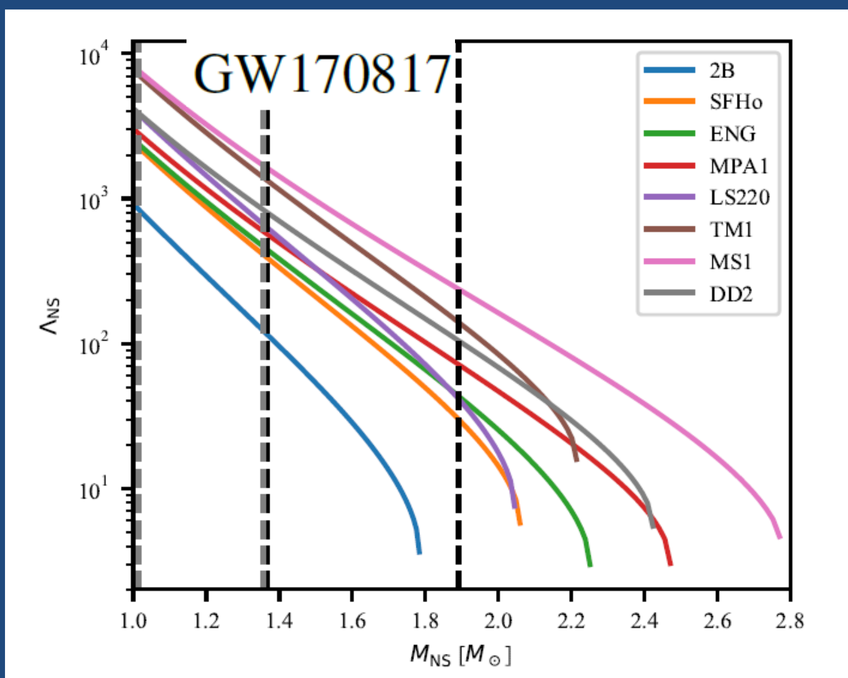

Barbieri+ 1908.08822

- $R_{tid} \sim R_{ns}(M_{bh}/M_{ns})^{1/3}$
  Mass shedding if
  $R_{tid} > R_{ISCO}$
- Depends on NS compactness $C = M_{ns}/R_{ns}$ (EOS)
- **Tidal parameter $\Lambda = 2k_2/(3C^5)$**
- Depends on the BH spin

Coalescing BH/NS mass ratio

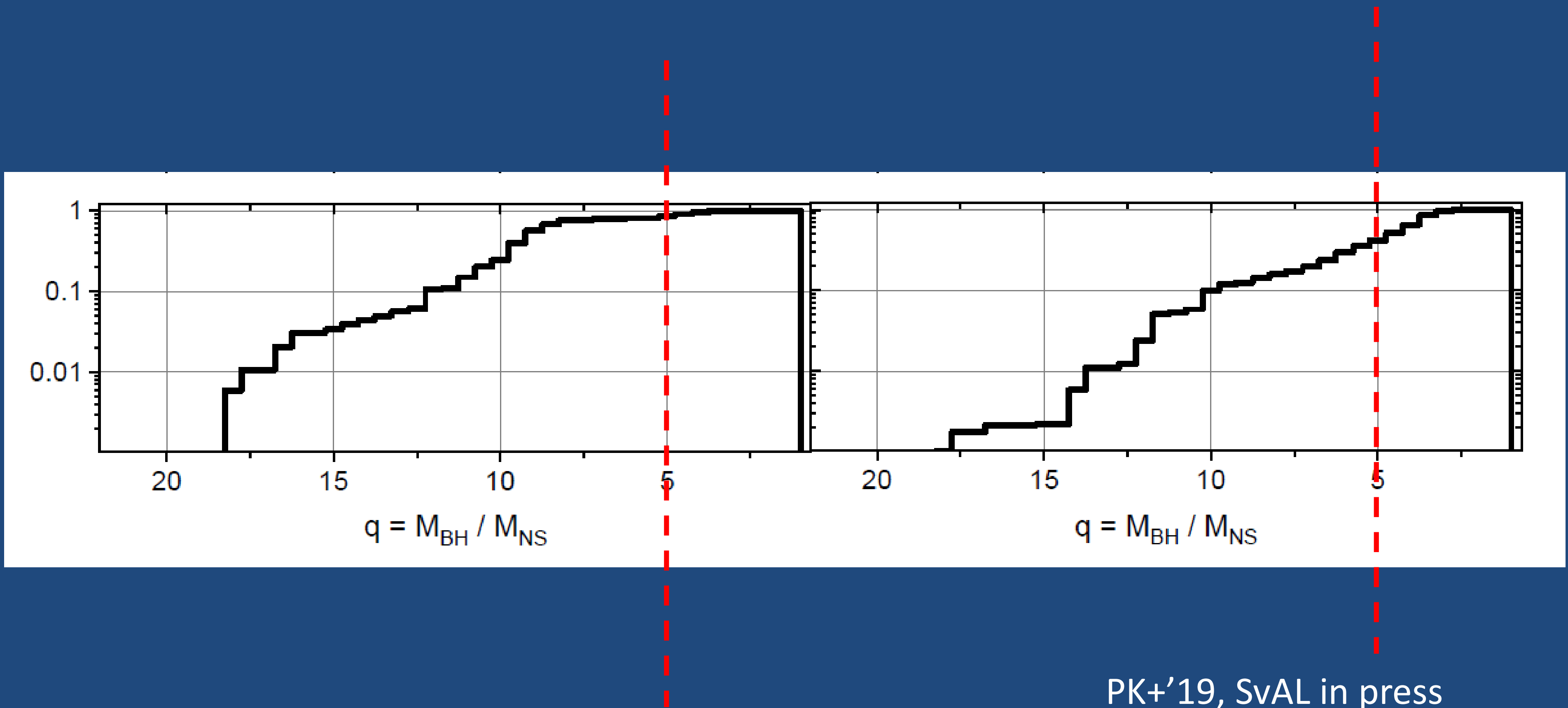

PK+'19, SvAL in press

10-30% of BH+NS coalescences can be tidally disrupted

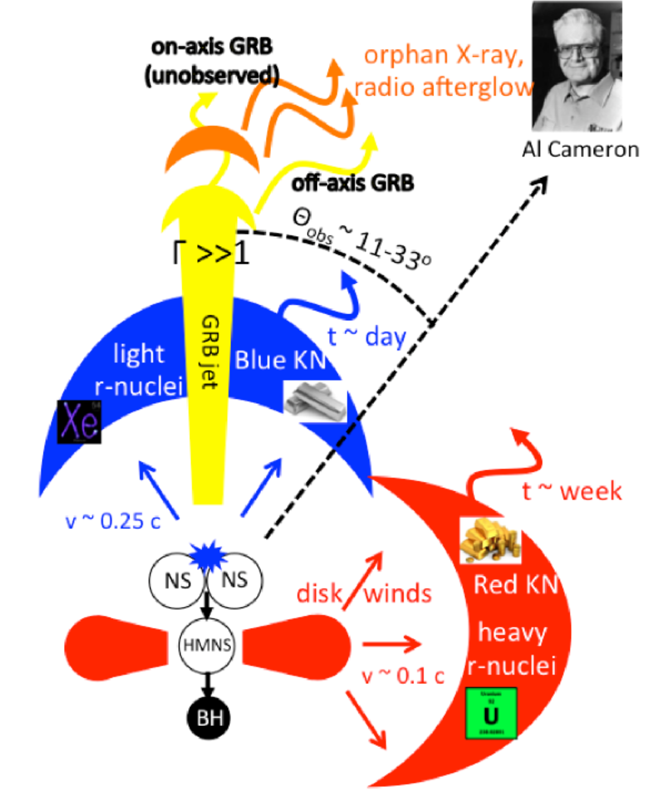

Mass ejection

- 'Dynamical' (merger) + 'viscous' (disc)

$$Y_e = \frac{n_e}{n_p + n_n} = \frac{n_p}{n_p + n_n}$$

Type of binary	Remnant	$M_{\rm ej,dyn}$	$M_{\rm ej,vis}$	$Y_{e,\rm dyn}$	$Y_{e,\rm vis}$	$\langle v_{\rm ej}\rangle$
Low-m BNS	SMNS	$O(10^{-3})$	$O(10^{-2})$	0.05–0.5	0.3–0.5	0.15
Mid-m BNS (stiff EOS)	HMNS	$O(10^{-3})$	$O(10^{-2})$	0.05–0.5	0.2–0.5	0.15
Mid-m BNS (soft EOS)	HMNS	$\sim 10^{-2}$	$O(10^{-2})$	0.05–0.5	0.2–0.5	0.20
High-m BNS ($q \sim 1$)	BH	$< 10^{-3}$	$< 10^{-3}$	—	—	—
High-m BNS ($q \ll 1$)	BH	$O(10^{-3})$	$\lesssim 10^{-2}$	0.05–0.1	0.05–0.3	0.30
BH-NS	BH	0–0.1	0–0.1	0.05–0.1	0.05–0.3	0.30

1908.02350

- **Mass ejection depends on the total mass M before the coalescence, binary mass ratio, component spins and tidal deformation (EOS)**
- Final BH mass and spin, emitted GW energy
  ➔ from numerical relativity simulations (Jimenez-Forteza+'18)
- Account for NS EOS ➔ from NR simulations of BH+NS mergings (Zappa+'19)

Final spin of BH

Initial BH spin from population synthesis (PK+'19)

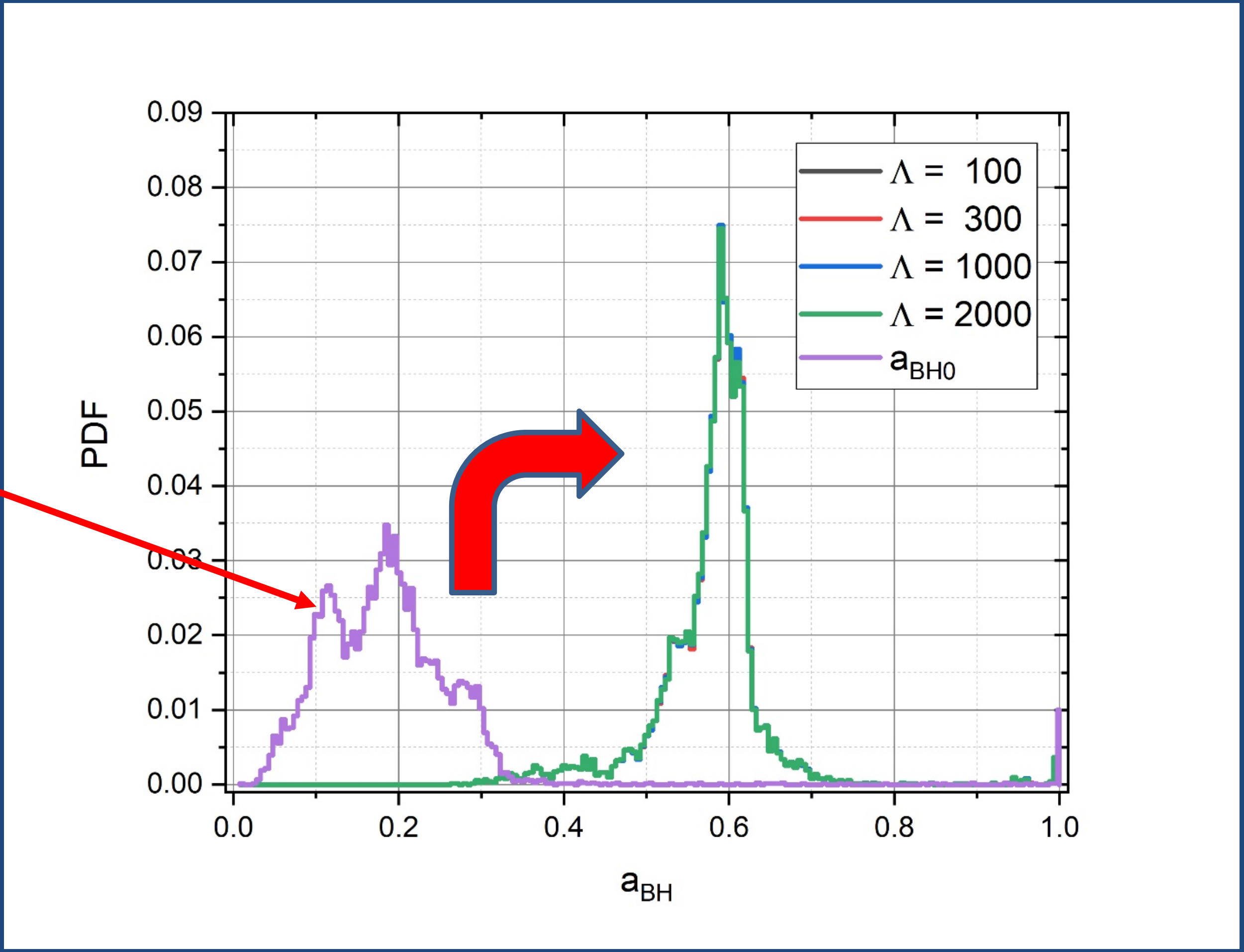

Final BH spin is almost insensitive to uncertain NS EOS!

Residual disk mass

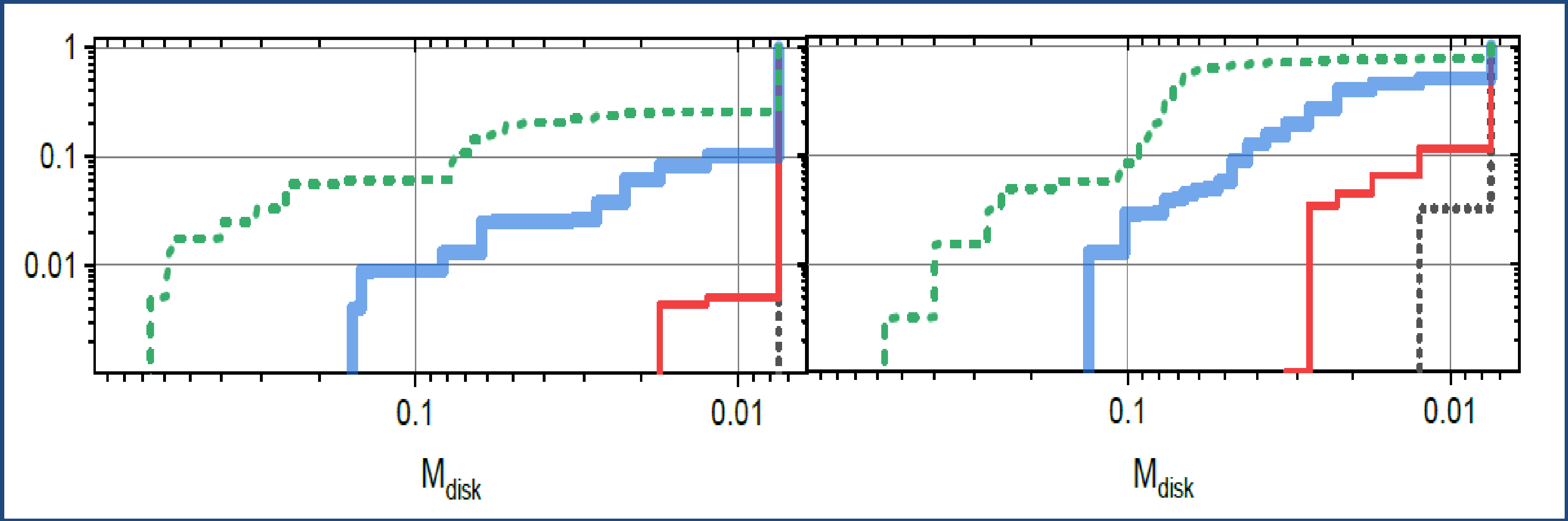

PK+'19, SvAL in press

- M_{disk} is determined by the mass ratio
- **Strongly depends on NS EOS!**
- Only large deformations (hard EOS) with **Λ>1000** can give rise to interesting disk masses

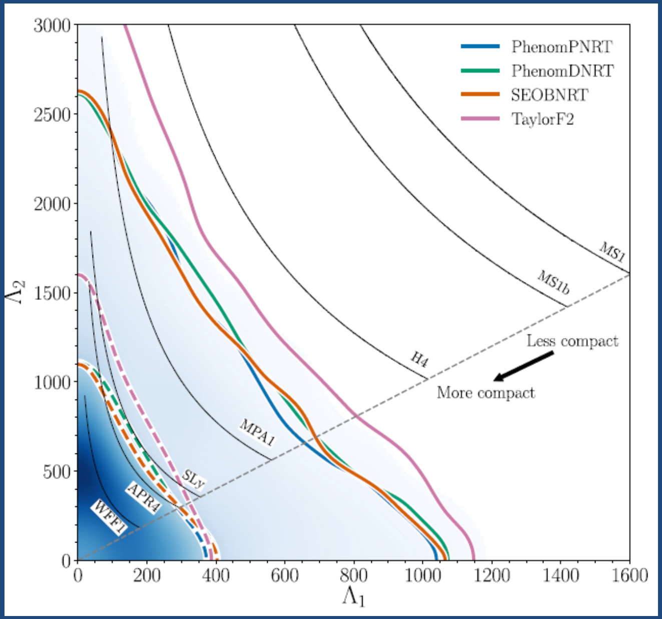

Constraints from GW170817:
~200<Λ< ~1600

1805.11579

BZ jet

$$L_{BZ} \sim B_d{}^2 M^2 \Omega_H^2 f(\Omega_H)$$

$$B^2 \sim \dot{M}_{accr} / M^2$$

$$\dot{M}_{accr} \sim M_{disk} / t_{accr}$$

$$E_{BZ} = \varepsilon M_{disk} \Omega_H^2 f(\Omega_H)$$

$$\varepsilon = 0.015 \quad (Barberi + '19)$$

BZ jet kinetic energy

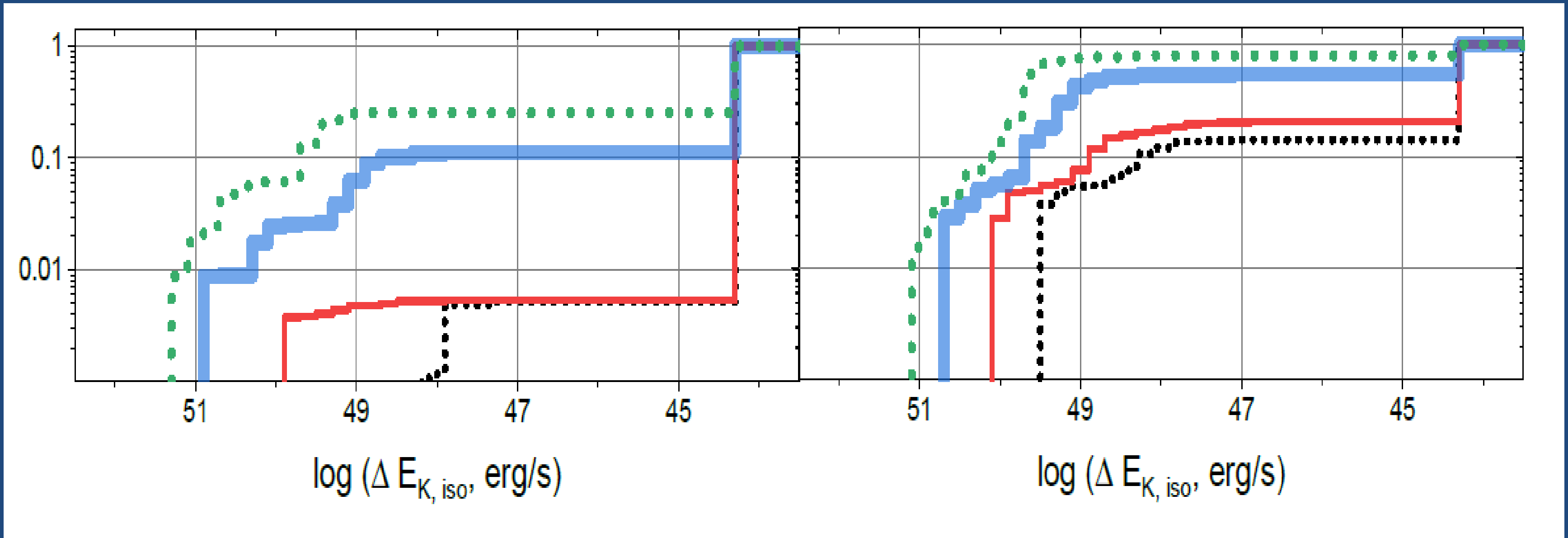

NS plunging into BH (q>5)

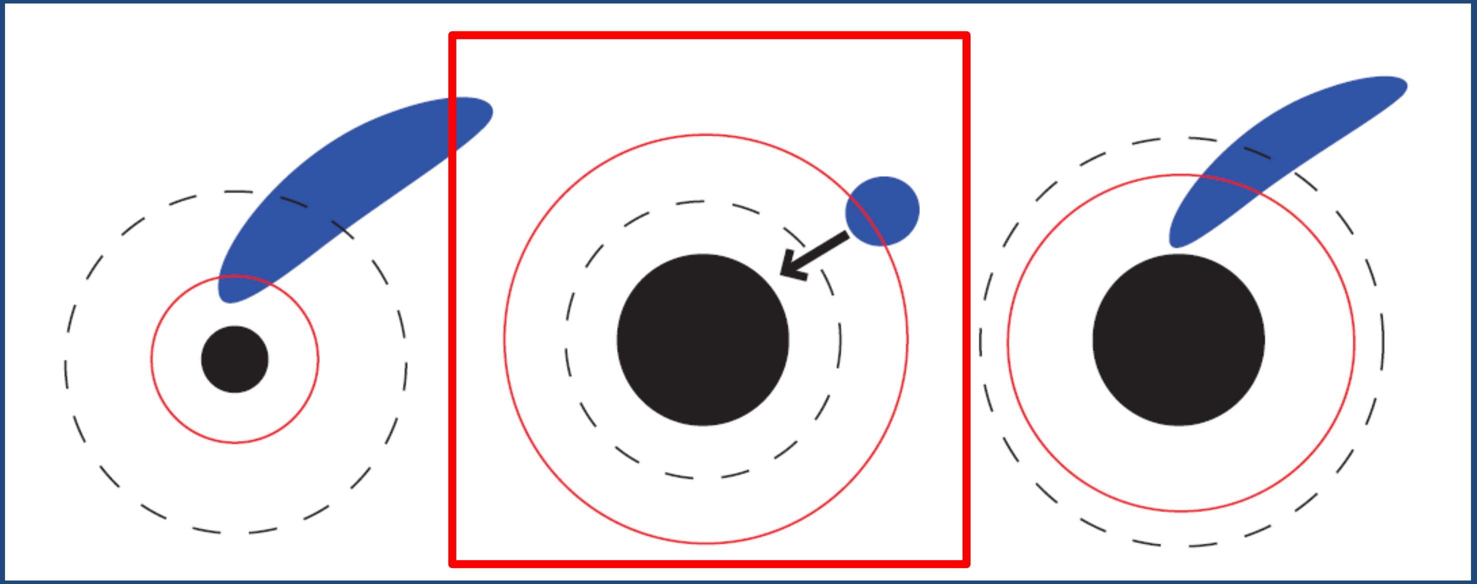

NS plunging into BH (q>5)

- A rotating BH in a magnetic field can acquire electric charge (Wald 1974)

$$
\begin{aligned}
Q_{\mathrm{W,max}} &\simeq \frac{2G}{c^3} J \times B_{\mathrm{S,NS}} = \frac{2G^2}{c^4} a M^2 B_{\mathrm{S,NS}} \\
&= 4.4 \times 10^{24} a \left(\frac{M}{10 M_{\odot}} \right)^2 \frac{B_{\mathrm{S,NS}}}{10^{12}\mathrm{G}} \ \mathrm{e.s.u.},
\end{aligned}
$$

- There can be EM emission associated with charged BH (Levin+’18, Shu-Quing Zhong+’19…)

NS rotation and magnetic field before the coalescence

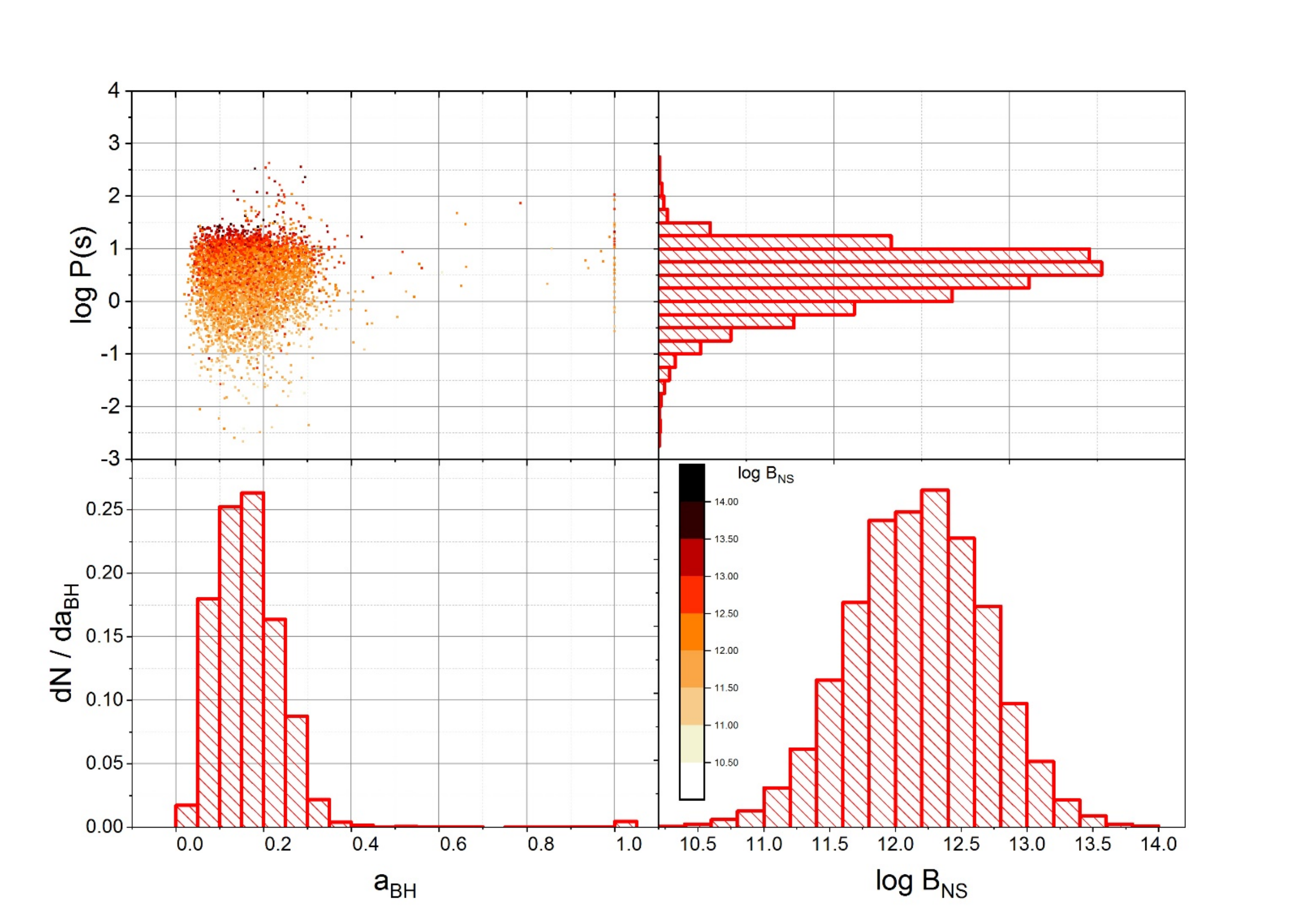

Wald BH charge

$Q_w = (2G/c^3)JB$ $J = a^* G M_{BH}^2 / c$ $Q_{RN} = 2\sqrt{G} M_{BH} \approx 10^{30} (M_{BH}/M_\odot)$

$$\tilde{q}_W = \frac{a^* b}{\sqrt{4\pi\alpha}} \left(\frac{m_e}{m_{Pl}}\right)^2 \left(\frac{M_{BH}}{m_{Pl}}\right) \approx 10^{-6} a^* b \left(\frac{M_{BH}}{M_\odot}\right)$$

Dimensionless Wald charge

$$\mu_{W,max} = \frac{J_{BH} Q_{W,max}}{M_{BH} c} \approx 5 \times 10^{30} a^{*2} b_s \left(\frac{R_{NS}}{10\text{км}}\right)^3$$

BGH dipole magnetic moment due to Wald charge before coalescence

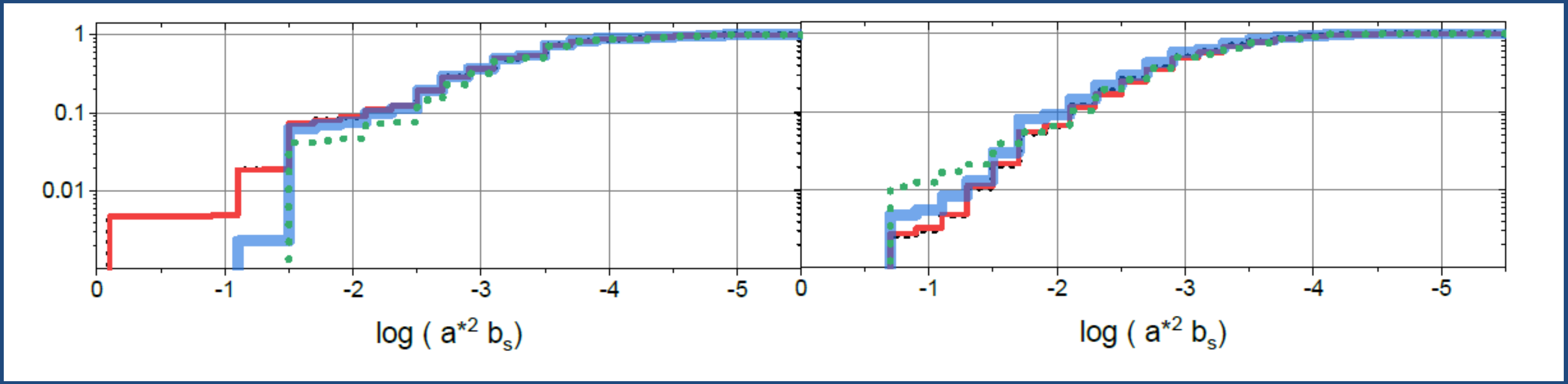

Maximum EM luminosity of BH after coalescence

$$L_{W,max} \sim 10^{42}[\text{эрг}/\text{с}] a^{*4} b_s^2 a_f^{*4} \frac{(R_{NS}/10\text{км})^6}{(M_{BH}^f/10M_\odot)^4}$$

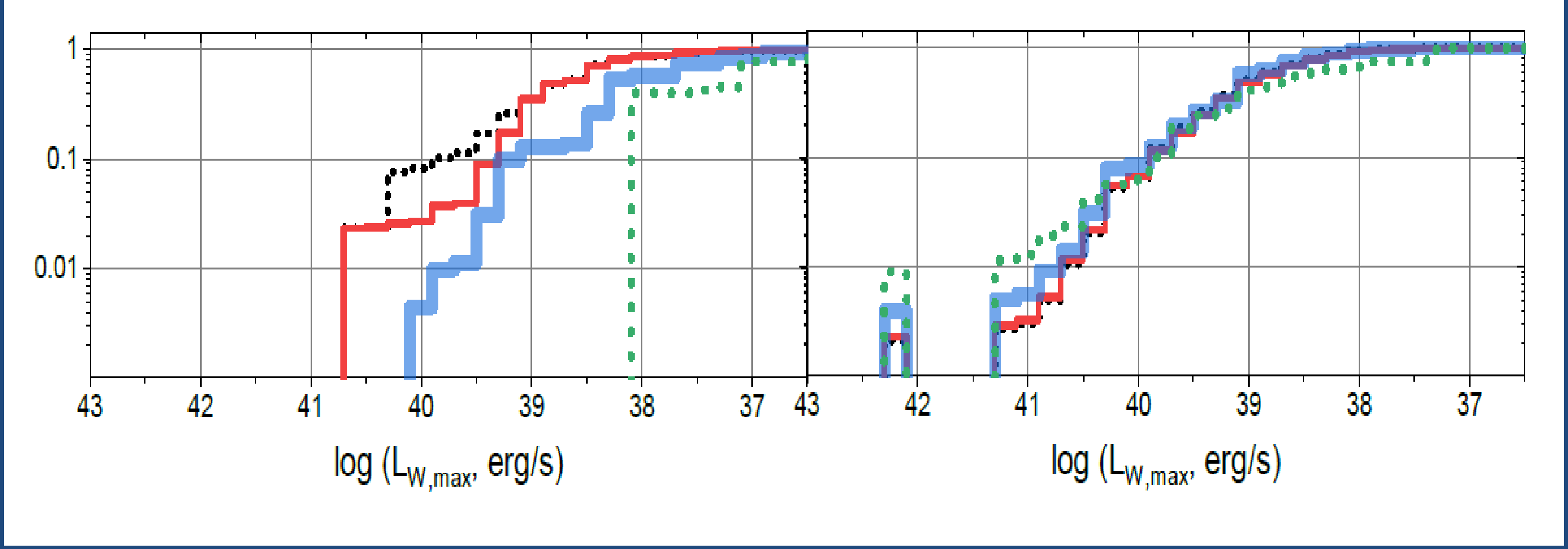

Takeaway messages:

- NS+BH rate is one order of magnitude smaller than BH+BH rate, ~ a few is expected within LVC O3 detection horizon (as of 19/10/19, 4 candidates out of 33 detections)
- Disk formation form NS tidal disruption mostly depends on (uncertain) NS EOS
- **1-10 % of NS+BH coalescences with tidally disrupted NS can launch relativistic BZ jets and produce short (likely subluminous) GRBs**
- More exotic (but less secure) mechanisms of EM radiation from high-mass-ratio NS+BH plunges are not excluded

3. Massive BH+BH: New physics ?

- Stellar-mass primordial black holes:
  - Can be formed in the early Universe in different models (Carr, Hawking'74)
  - Can be in binaries (Nakamura+'97)
  - Can naturally explain low spins of observed BH+BH (Bird+'16, Blinnikov+'16,…)
  - Can substantially contribute to dark matter
  - Can be seeds for growth of SMBH in galactic centers

Particular model: primordial BH in the modified supersymmetric baryogenesis scenario (Affleck-Dine mechanism)

- Dolgov + (1993, 2009): inflation field coupled with renormalizable scalar baryon field

$$U(\chi, \Phi) = U_\Phi(\Phi) + U_\chi(\chi) + \lambda_1(\Phi - \Phi_1)^2|\chi|^2,$$

- High-B bubbles with almost model-independent mass distribution

$$\frac{dn}{dM} = C \exp\left[-\gamma \ln^2(M/M_{\max})\right]$$

- Small-scale B –number fluctuations originally are isocurvature perturbations, but after QCD phase transition @ 100-200 MeV are transformed into large density perturbations at astrophysically large but cosmologically small scales (Dolgov, Silk, **PRD47 (1993) 4244**)

- High-B bubbles could form **primordial BHs**, compact stellar-mass objects or dense primordial gas clouds. Primordial BHs can be seeds for early galaxy formation (Dolgov+ Nucl.Phys. B807 (2009) 229, Dolgov, Blinnikov PRD89 (2014) 021301,Carr,Silk 2019…)

Estimate of mass distribution

$$\varrho_c = 1.4 \times 10^{11} M_\odot \mathrm{Mpc}^{-3}$$

$$\varrho_m = 4 \times 10^{10} M_\odot \mathrm{Mpc}^{-3}$$

$$\frac{dn}{dM} = \mu^2 \exp\left[-\gamma \ln^2(M/M_{max})\right]$$

$$\mu = \mu_{43} \times 10^{-43} / \ \mathrm{Mpc}$$

(in units c=h=1)

- A. Fraction of DM in MACHOs is 0.1 for mass range 0.1-1 Msun
- B. Primordial BH make up to all cosmological DM
- C. Density of primordial BH with M> 10^4 = density of observed large galaxies

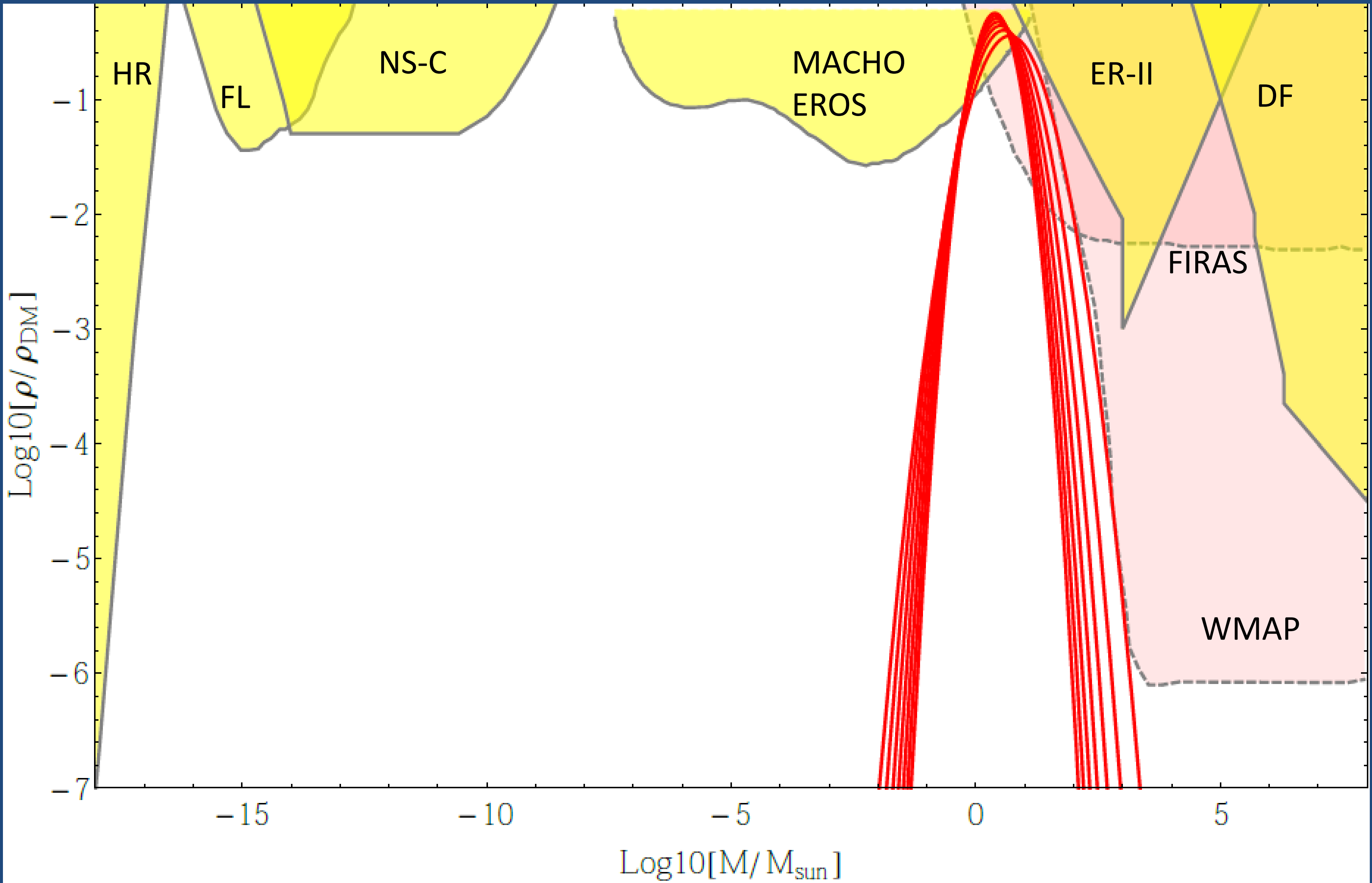

Blinnikov, Dolgov, PK, Porayko 2016 JCAP 11 036

Present constraints (model-dependent)

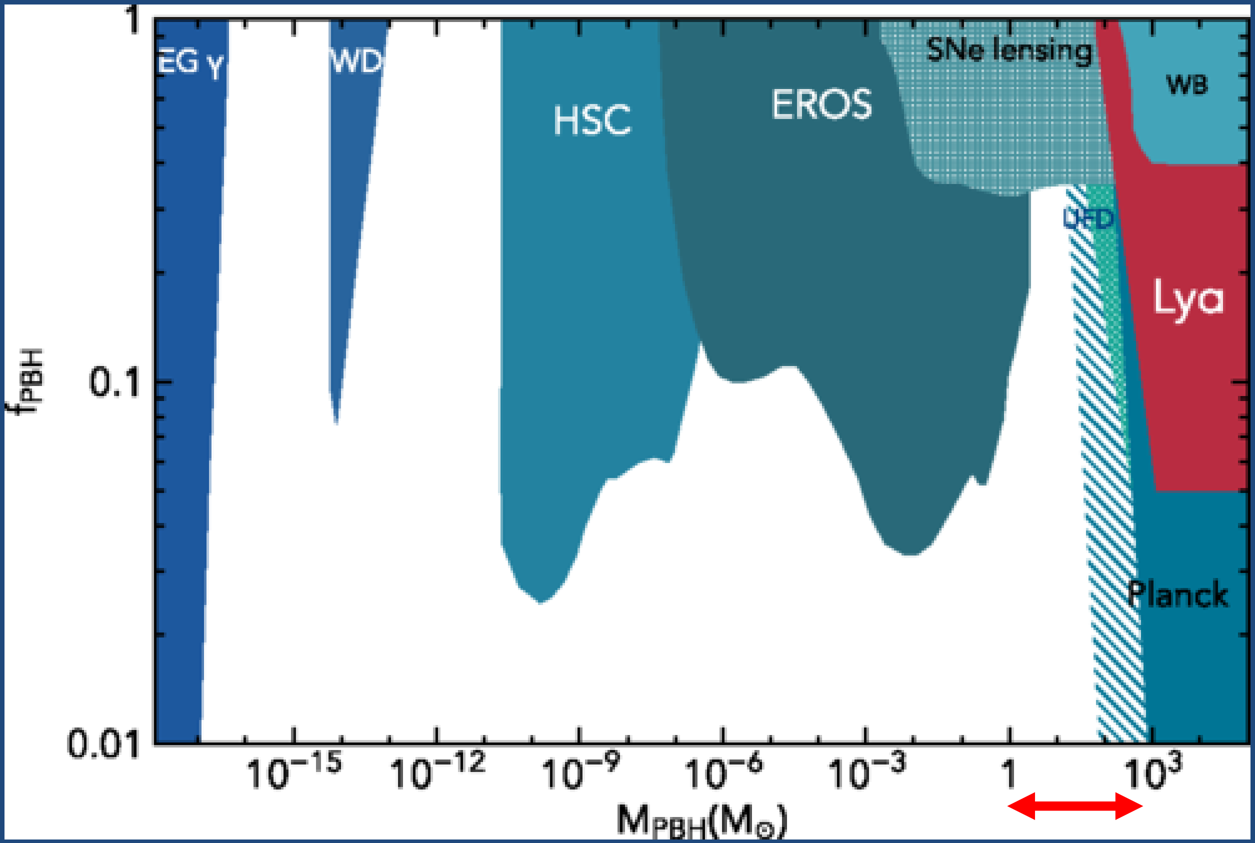

1-100 M☉ PBH are still in the open window!

Murgia+’19

Fraction of PBH mergings with M>100 $M_\odot$

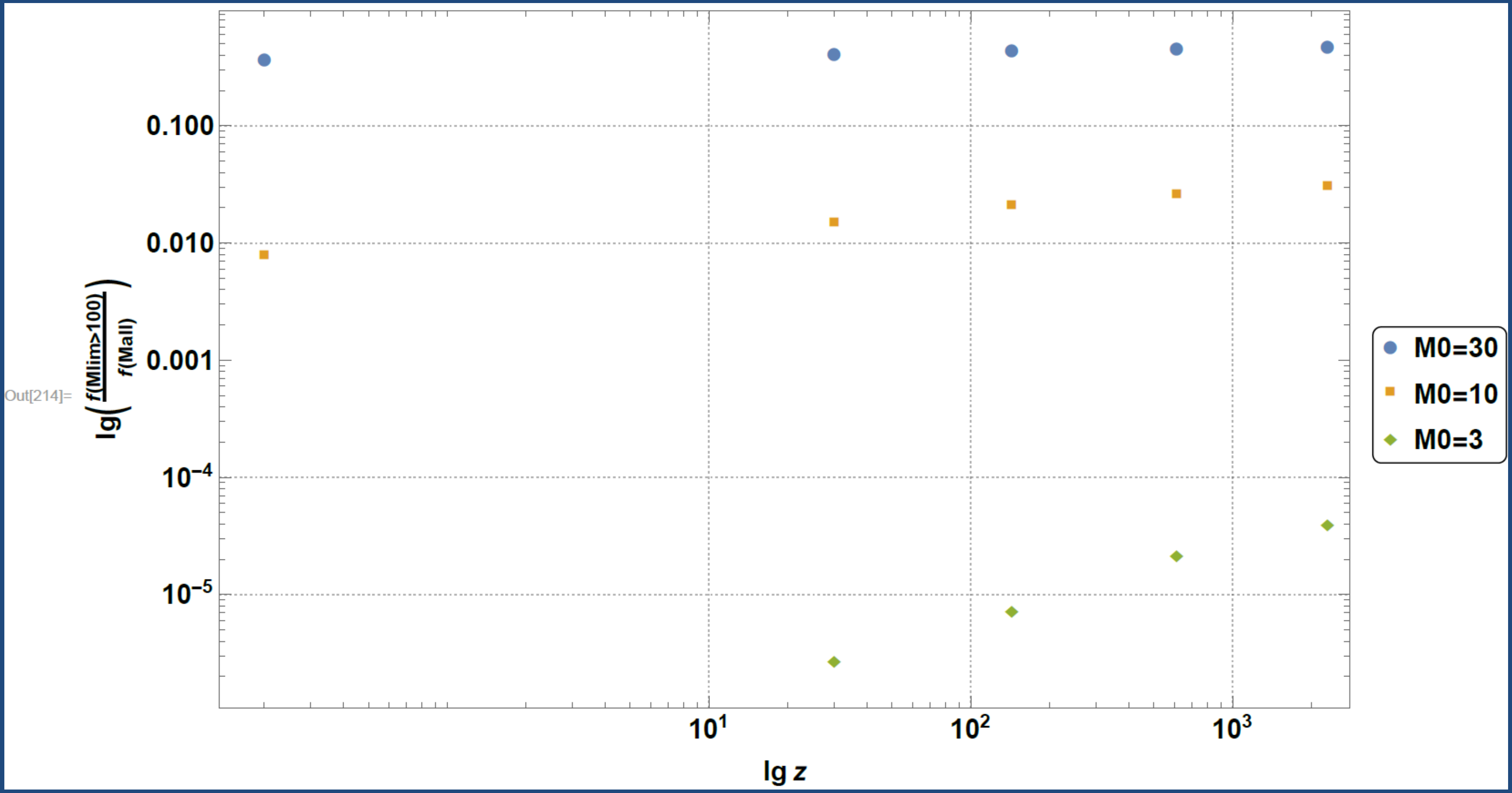

1/100-1/1000 for log-normal PBH mass distribution with M_0~5-10 $M_\odot$

(PK+ in preparation)

GW road map (official)

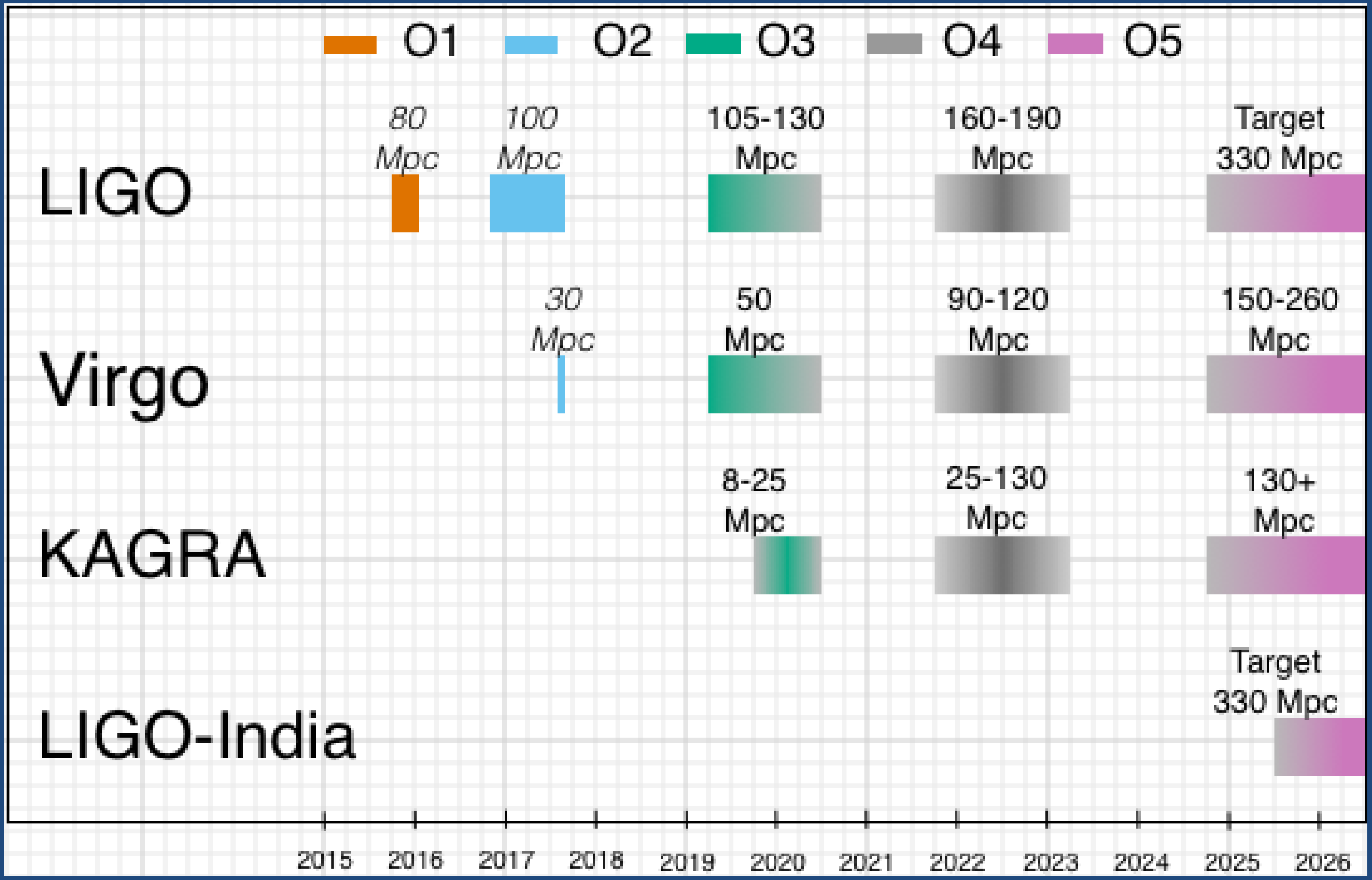

Conclusions

- BH+BH coalescences became routine (once per a few days) GW detections
- Masses and spins of (confirmed) BH+BH can be adequately explained by the standard astrophysical formation from massive binary star evolution
- Primordial stellar mass BHs among detected sources are not ruled out. Detection of ~100 $M_\odot$ BH (tbc) would challenge astrophysical explanation and may point to other BH formation channels (PopIII? PBH?)
- First O3 LVC publications by the end of this year – stay tuned!